Atmospheric Research 206 (2018) 87–107

Contents lists available at ScienceDirect

Atmospheric Research

journal homepage: www.elsevier.com/locate/atmosres

Future projections of temperature and precipitation climatology for CORDEX-MENA domain using RegCM4.4

Tugba Ozturk[a,d,*], M. Tufan Turp[b,d], Murat Türkeş[d], M. Levent Kurnaz[c,d]

[a] Department of Physics, Faculty of Arts and Sciences, Isik University, 34980 Istanbul, Turkey
[b] Department of Environmental Sciences, Institute of Environmental Sciences, Bogazici University, 34342 Istanbul, Turkey
[c] Department of Physics, Faculty of Arts and Sciences, Bogazici University, 34342 Istanbul, Turkey
[d] Center for Climate Change and Policy Studies, Bogazici University, 34342 Istanbul, Turkey

ARTICLE INFO

Keywords:
Arid-lands
Climate change
Middle East
Central and North Africa
Regional climate modeling
RegCM4.4
Projections

ABSTRACT

In this study, we investigate changes in seasonal temperature and precipitation climatology of CORDEX Middle East and North Africa (MENA) region for three periods of 2010–2040, 2040–2070 and 2070–2100 with respect to the control period of 1970–2000 by using regional climate model simulations. Projections of future climate conditions are modeled by forcing Regional Climate Model, RegCM4.4 of the International Centre for Theoretical Physics (ICTP) with two different CMIP5 global climate models. HadGEM2-ES global climate model of the Met Office Hadley Centre and MPI-ESM-MR global climate model of the Max Planck Institute for Meteorology were used to generate 50 km resolution data for the Coordinated Regional Climate Downscaling Experiment (CORDEX) Region 13. We test the seasonal time-scale performance of RegCM4.4 in simulating the observed climatology over domain of the MENA by using the output of two different global climate models. The projection results show relatively high increase of average temperatures from 3 °C up to 9 °C over the domain for far future (2070–2100). A strong decrease in precipitation is projected in almost all parts of the domain according to the output of the regional model forced by scenario outputs of two global models. Therefore, warmer and drier than present climate conditions are projected to occur more intensely over the CORDEX-MENA domain.

1. Introduction

Climate change can be considered as one of the most significant challenges that the world has ever faced. According to the Fifth Assessment Report (AR5) of the Intergovernmental Panel on Climate Change (IPCC), warming in our climate system is explicit and since the 1950s unprecedented changes in climate have been observed for decades. During this period, the atmosphere and the oceans have gotten warmer, levels of snow and ice have diminished, the sea level has risen and the atmospheric greenhouse gas concentration has increased (IPCC, 2013a). Today, many aspects of our daily life are being affected by climate change. When the climatological, hydrological, biological and societal impacts of climate change are regarded, the studies which present projected climate change and its possible effects become crucial.

Since the effects of climate change exhibits varied characteristics in different domains and time scales, regional studies are very critical to detect the climate change signal properly. In this paper, we focus on the Middle East and North Africa (MENA) CORDEX domain (Evans, 2011; Giorgi et al., 2009). CORDEX-MENA is a large domain which comprises the entire Middle East and Mediterranean regions and also covers the northern part of Africa. MENA is more vulnerable to global climate change than those in other areas since it spans extensive arid, semi-arid, and hyper-arid areas of three different continents.

According to Evans (2009), it is expected that an increase of 1.4 °C in mean temperatures will occur for the period of 2045–2054 and this increase will likely reach 4 °C during the period of 2090–2099 in the Middle East region of MENA. The models also predict a decrease in the total amounts of precipitation over the Middle East because of weakening of the Eastern Mediterranean storm track (Evans, 2009, 2010). The significant reduction trend in precipitation over the MENA region will very likely lead relevant countries to face with severe water crisis (Alpert et al., 2008; Arnell, 2004; Conway and Hulme, 1996; Sowers et al., 2011). However, in the southernmost part of the Middle East, a slight increase in the total amount of precipitation can be seen associated with the shifting of the Inter Tropical Convergence Zone (ITCZ) towards the north (Evans, 2009). The observational analyses already found that the number of warm days have been increasing in the Middle East region, whereas the frequency of cold days have been decreasing (Zhang et al., 2005) respectively. Similarly, the studies about the

* Corresponding author at: Işık University, Department of Physics, Şile, 34980 İstanbul, Turkey.
E-mail address: tugba.ozturk@isikun.edu.tr (T. Ozturk).

https://doi.org/10.1016/j.atmosres.2018.02.009
Received 5 October 2017; Received in revised form 16 January 2018; Accepted 14 February 2018
Available online 16 February 2018
0169-8095/

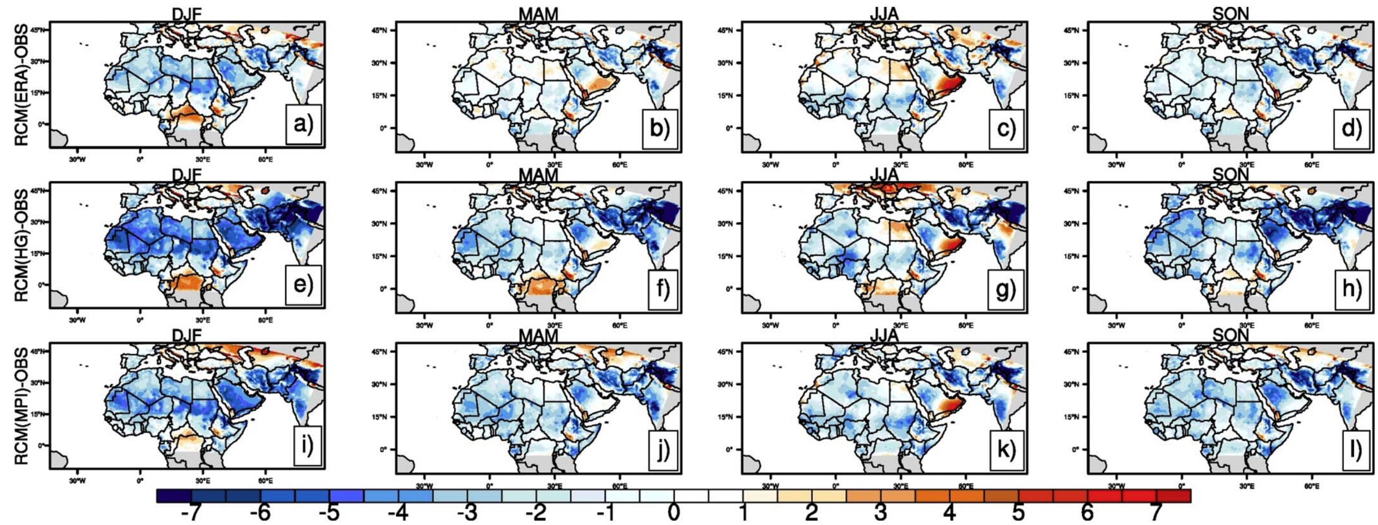

Fig. 1. Air temperature biases (°C) obtained from RegCM4.4 with ERA-interim dataset for the period 1980–2000: (a) winter, (b) spring, (c) summer and (d) autumn seasons; with the HadGEM2-ES dataset: (e) winter, (f) spring, (g) summer and (h) autumn seasons, and with the MPI-ESM-MR dataset: (i) winter, (j) spring, (k) summer and (l) autumn seasons for the period 1970–2000 with respect to CRU dataset. (Even though figures include the largest part of the Indian subcontinent, a few grid boxes were disregarded from the analysis.)

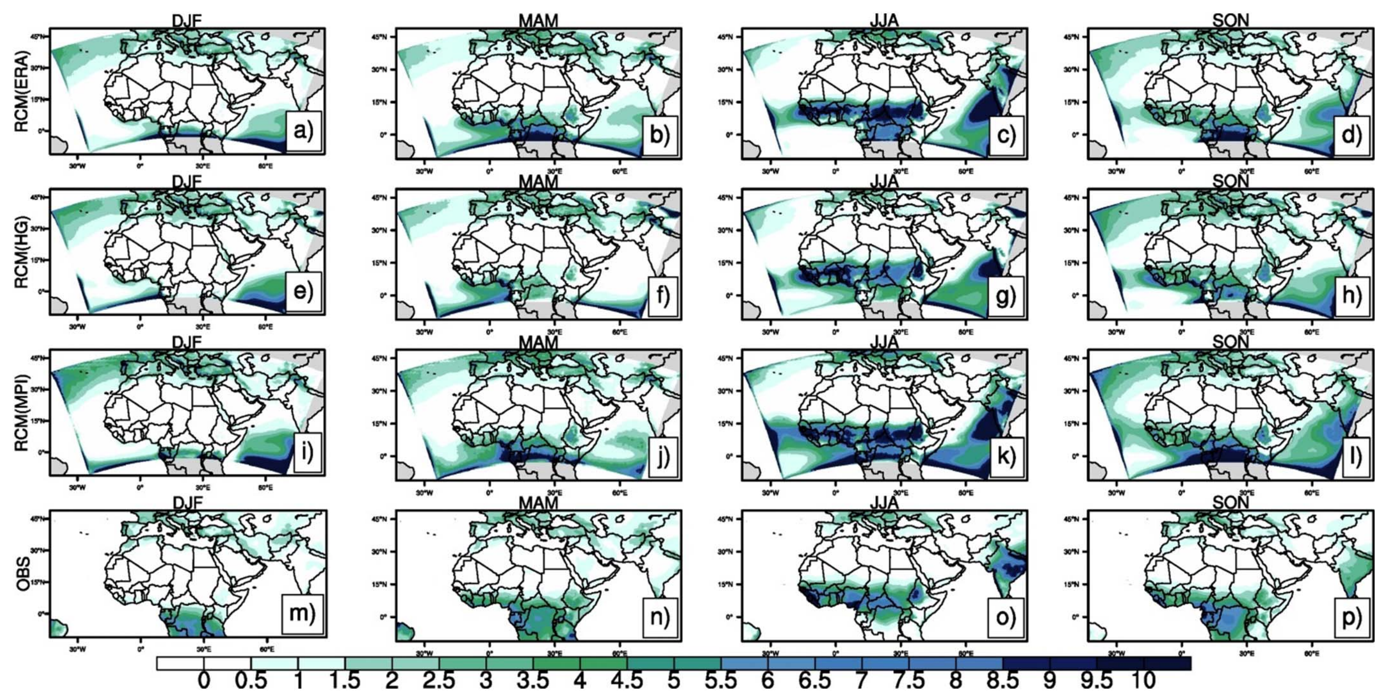

Fig. 2. Precipitation (mm/day) obtained from RegCM4.4 with ERA-interim dataset for the period 1980–2000: (a) winter, (b) spring, (c) summer and (d) autumn seasons; with the HadGEM2-ES dataset: (e) winter, (f) spring, (g) summer and (h) autumn seasons, and with the MPI-ESM-MR dataset: (i) winter, (j) spring, (k) summer and (l) autumn seasons for the period 1970–2000 with respect to CRU dataset. CRU observational precipitation dataset is for the period 1970–2000: (m) winter, (n) spring, (o) summer and (p) autumn seasons.

Mediterranean region including Turkey also indicated warmer and drier climate conditions during the current century (Adloff et al., 2015; Erlat and Türkeş, 2013, 2017; Gao and Giorgi, 2008; Giorgi, 2006; Giorgi and Lionello, 2008; Hertig and Jacobeit, 2008; Kutiel and Türkeş, 2017; Lelieveld et al., 2012; Somot et al., 2008; Tramblay et al., 2013; Turp et al., 2014, 2015). The results indicate that the frequency of extreme climatic conditions over the large Mediterranean Basin will also increase (Giorgi, 2006; Kuglitsch et al., 2010; Ozturk et al., 2011, 2015; Sánchez et al., 2004; Topcu et al., 2010; Türkeş et al., 2011). In other words, a warmer climate will enhance severe drought and flood events in the region. It is expected that mean temperatures of North Africa region will increase over time as well, while the amount of total annual precipitation will drop (Hulme et al., 2001; Paeth et al., 2009; Radhouane, 2013). The warming trend will be higher in boreal summer season (July–August–September) than boreal winter season (January–February–March) (Laprise et al., 2013). Although the model projections can show different precipitation patterns individually, their ensemble outcomes are reliable and they are accurate enough to provide

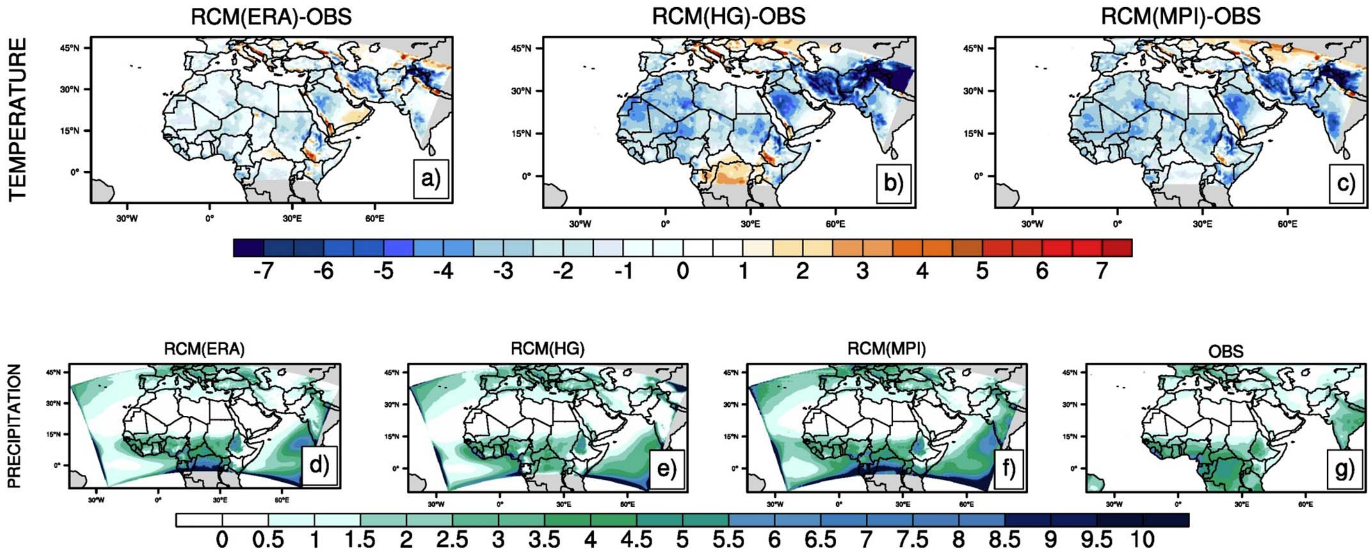

Fig. 3. Annual air temperature biases (°C) obtained from RegCM4.4 with (a) ERA-interim dataset for the period 1980–2000, (b) HadGEM2-ES dataset and (c) MPI-ESM-MR dataset for the period 1970–2000 with respect to CRU dataset. Annual precipitation (mm/day) values obtained from RegCM4.4 with (d) ERA-interim dataset for the period 1980–2000, (e) HadGEM2-ES dataset, (f) MPI-ESM-MR dataset for the period 1970–2000 and (g) annual CRU observational precipitation dataset for the period 1970–2000.

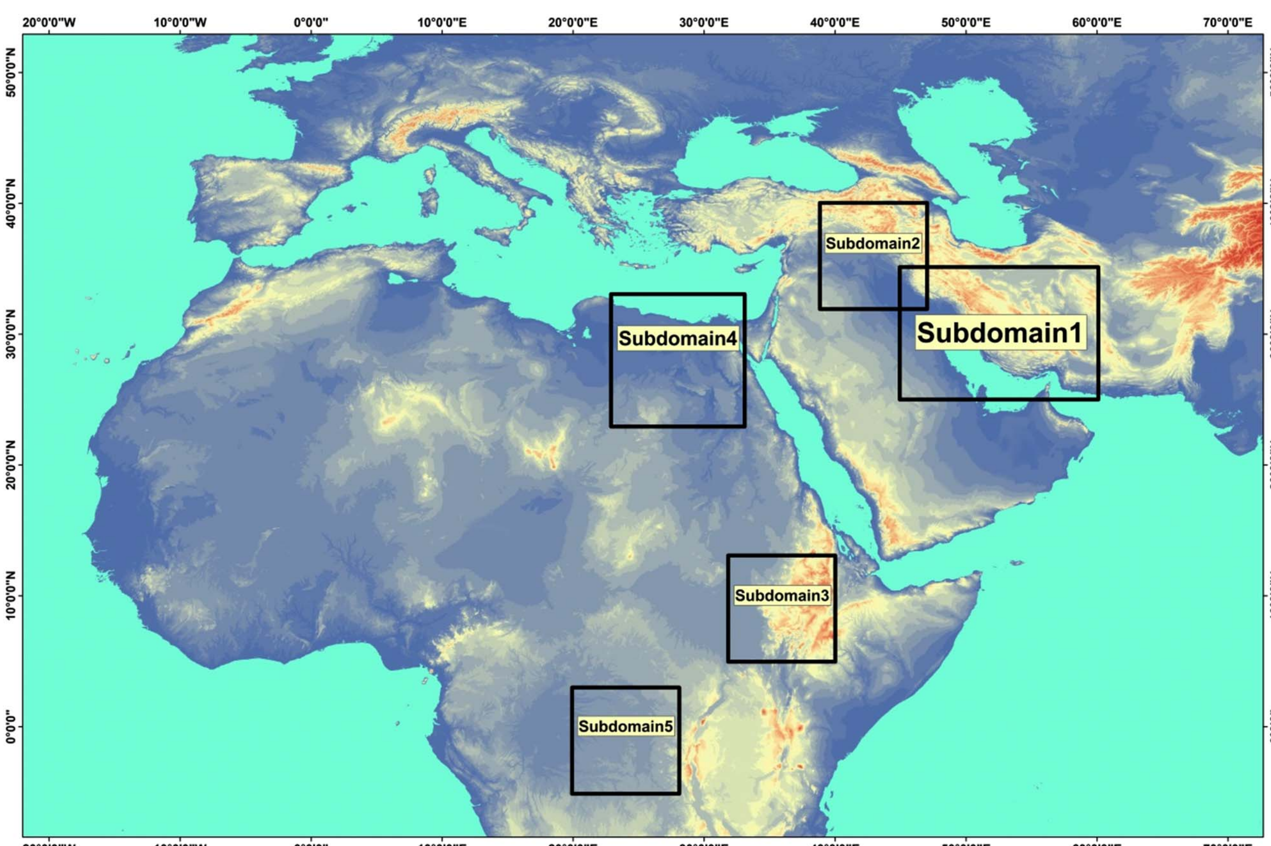

Fig. 4. General physical/relief map of CORDEX-MENA Region, subdomains delimitated for the study and its surroundings.

future projections about the climate of North Africa (Laprise et al., 2013; Nikulin et al., 2012; Radhouane, 2013). Considering North Africa's arid, semi-arid, and hyper-arid areas, the vulnerability of the North Africa domain to global climate change can cause serious problems in terms of water availability and access to clean water.

A recent research about the CORDEX-MENA domain, which was done by Almazroui (2016), focuses on the selection of the most reliable domain and schemes for the simulations via the regional climate model called RegCM4 (Regional Climate Model version 4) of the Abdus Salam International Center for Theoretical Physics (ICTP). Besides, Almazroui

Table 1
Some statistics for seasonal temperature (°C) series weighted over the whole domain and subdomains for the reference periods of 1980–2000 for ERA-Interim, and 1970–2000 for GCMs and RegCM.

Whole domain		ERA	RegCM_ERA	GCM_MPI	RegCM_MPI	GCM_HadGEM2	RegCM_HadGEM2
SON	Bias	−0.027	−1.097	0.081	−2.078	−1.764	−2.275
	RMSE	1.298	1.916	1.839	2.709	2.878	3.278
	Correlation	0.975	0.966	0.949	0.956	0.921	0.935
DJF	Bias	−0.157	−1.306	−0.815	−2.247	−2.626	−2.834
	RMSE	1.239	2.477	2.565	3.250	3.718	3.996
	Correlation	0.991	0.974	0.969	0.966	0.958	0.959
MAM	Bias	0.043	−0.494	0.130	−1.919	−1.210	−1.676
	RMSE	1.343	1.588	1.768	2.583	2.515	2.858
	Correlation	0.981	0.978	0.968	0.969	0.949	0.951
JJA	Bias	0.263	−0.482	0.767	−1.614	−0.482	−1.170
	RMSE	1.590	2.066	2.157	2.521	2.260	2.751
	Correlation	0.960	0.929	0.931	0.931	0.891	0.883
Subdomain 1							
SON	Bias	1.031	−2.399	0.354	−3.662	−2.832	−5.023
	RMSE	1.557	3.402	2.237	4.322	3.757	5.456
	Correlation	0.970	0.911	0.888	0.915	0.864	0.934
DJF	Bias	0.054	−2.337	−0.309	−3.283	−3.745	−4.342
	RMSE	1.132	3.096	2.009	3.840	4.586	4.912
	Correlation	0.976	0.923	0.920	0.925	0.862	0.908
MAM	Bias	0.630	−1.325	−0.276	−2.783	−1.025	−3.367
	RMSE	1.510	2.500	2.161	3.449	2.547	4.105
	Correlation	0.966	0.922	0.897	0.925	0.867	0.920
JJA	Bias	1.552	−0.652	1.462	−2.123	−0.559	−2.861
	RMSE	2.067	2.504	3.011	3.335	2.885	4.076
	Correlation	0.944	0.874	0.779	0.865	0.705	0.870
Subdomain 2							
SON	Bias	0.083	−1.352	0.144	−2.413	−3.208	−3.874
	RMSE	1.134	1.974	1.689	2.765	3.710	4.077
	Correlation	0.982	0.969	0.949	0.970	0.959	0.974
DJF	Bias	0.128	−1.216	1.142	−1.596	−2.421	−2.163
	RMSE	1.281	2.159	2.568	2.332	3.950	2.781
	Correlation	0.983	0.974	0.950	0.977	0.952	0.977
MAM	Bias	0.191	−0.736	0.498	−1.391	−1.199	−1.978
	RMSE	1.139	1.645	1.727	1.955	2.127	2.434
	Correlation	0.986	0.971	0.959	0.974	0.961	0.974
JJA	Bias	0.636	−0.222	−0.417	−1.398	−1.518	−1.344
	RMSE	1.667	1.742	2.443	2.289	2.348	2.144
	Correlation	0.977	0.959	0.933	0.962	0.940	0.964
Subdomain 3							
SON	Bias	−0.684	0.072	0.289	−1.201	−0.534	−0.260
	RMSE	1.707	1.980	1.559	2.209	1.752	2.556
	Correlation	0.959	0.920	0.947	0.929	0.936	0.892
DJF	Bias	−0.040	0.246	−0.614	−1.360	−0.399	−0.802
	RMSE	1.479	2.493	1.621	2.827	1.774	2.846
	Correlation	0.952	0.860	0.948	0.861	0.936	0.839
MAM	Bias	−0.583	−0.097	1.027	−1.655	0.629	0.187
	RMSE	1.524	2.198	1.866	2.850	1.910	2.642
	Correlation	0.970	0.906	0.951	0.896	0.938	0.874
JJA	Bias	−0.934	−1.425	0.467	−2.613	0.112	−0.575
	RMSE	1.750	2.606	1.621	3.181	1.703	2.663
	Correlation	0.943	0.872	0.944	0.910	0.920	0.869
Subdomain 4							
SON	Bias	0.262	−1.145	−0.428	−1.719	−2.088	−1.115
	RMSE	0.542	1.251	0.780	1.787	2.290	1.232
	Correlation	0.920	0.912	0.853	0.918	0.672	0.900

(continued on next page)

Table 1 (*continued*)

Subdomain 4							
DJF	Bias	−0.172	−2.192	−1.423	−2.457	−2.525	−3.069
	RMSE	0.613	2.261	1.595	2.509	2.742	3.109
	Correlation	0.790	0.792	0.663	0.829	0.475	0.840
MAM	Bias	0.771	0.819	−0.126	−0.145	−1.425	−0.119
	RMSE	0.913	1.026	0.737	0.676	1.686	0.648
	Correlation	0.967	0.948	0.952	0.954	0.882	0.954
JJA	Bias	0.935	1.729	0.677	0.317	−1.028	1.937
	RMSE	1.122	1.827	1.242	0.833	1.613	2.101
	Correlation	0.942	0.949	0.827	0.914	0.741	0.897

Subdomain 5							
SON	Bias	−1.961	−1.899	−0.825	−1.710	−0.473	0.732
	RMSE	1.988	1.923	0.991	1.882	0.780	1.186
	Correlation	0.853	0.859	0.813	0.515	0.804	0.486
DJF	Bias	−1.973	1.002	−1.079	1.219	−0.390	3.587
	RMSE	2.026	1.893	1.341	1.372	0.815	3.639
	Correlation	0.826	0.395	0.770	0.714	0.852	0.741
MAM	Bias	−1.899	−1.402	−0.242	−0.711	0.632	3.269
	RMSE	1.928	1.479	1.130	1.158	1.135	3.319
	Correlation	0.881	0.724	0.596	0.222	0.782	0.658
JJA	Bias	−1.179	−1.113	0.059	−1.285	0.992	1.850
	RMSE	1.269	1.291	0.644	1.774	1.259	2.027
	Correlation	0.810	0.672	0.717	0.358	0.829	0.589

et al. (2015) carried out a research which analyses the best convective parameterization scheme to downscale the data of Coupled Model Intercomparison Project Phase 5 (CMIP5) dynamically via RegCM4 for the CORDEX-MENA domain. Similarly, Zittis et al. (2014) investigated the performance of different physical parameterizations within the climate version of Weather Research and Forecasting (WRF) Model over the CORDEX-MENA domain. In another recently published work, Bucchignani et al. (2016) evaluated the sensitivity of the non-hydrostatic regional climate model COSMO-CLM, which is developed by the Climate Limited-area Modeling (CLM) Community, over CORDEX-MENA domain.

The MENA domain, which includes the Mediterranean Basin, Middle East and North Africa is a region of great interest when it comes to future climate predictions, given its transitional climate setting and geo-political situation. Since the MENA region is a relatively recently established CORDEX domain within the 14 regions in CORDEX, the number of climate change studies related to this domain needs to be increased. The intense warming and the increase in the severity and frequency of extreme climate events that can be seen in the MENA region, one of the world's hottest and driest climatic conditions, will pose a serious threat to millions of people in terms of agriculture, food safety, water access and health (Lelieveld et al., 2014, 2016; Tanarhte et al., 2015). In order to be prepared for this threat and to be able to adapt to changing climate, studies involving future projections of the region play a valuable role. In this context, this work will be one of the first contributions of future projections based on the RCP scenarios and the CMIP5 global model datasets.

In this study, we aim at providing useful information about the changes in two fundamental climate variables, temperature and precipitation, for a wide domain including the Mediterranean Basin, Middle East, and North Africa by way of a dynamical downscaling approach based on RCP4.5 and RCP8.5 scenarios. The paper is organized as follows: In Section 2, data, climate models and statistical methods used in the study are described. In Section 3 in general, results of the analysis are presented. In this respect, in the Section 3.1, performance of the regional climate model in simulating observed climate of the region by using ERA-Interim reanalysis dataset and global climate models of HadGEM2-ES and MPI-ESM-MR as a forcing data to the model is investigated. Results of the temperature and precipitation projections for three future periods of 2010–2040, 2040–2070 and 2070–2100 with respect to the present period of 1970–2000 based on the IPCC's RCP4.5 and RCP8.5 emission scenarios are evaluated in the Section 3.2. Finally, in the last section, conclusions and discussions of the results are developed.

2. Data and model description

RegCM has been effectively applied to several domains (i.e. the Mediterranean, Africa, North America, Central America, South America, East Asia, Central Asia, South Asia, Europe) in a variety of regional climate change and climate variability studies (e.g. Almazroui, 2012, 2016; Almazroui et al., 2016, 2017; Chen et al., 2003; Coppola et al., 2014; Gao et al., 2002; Giorgi, 2014; Giorgi et al., 2004a, 2004b, 2012, 2014; Gu et al., 2012; Ji and Kang, 2013; Ji et al., 2015, 2016a; Maity et al., 2017; Mariotti et al., 2014; Ozturk et al., 2011, 2012; Salih et al., 2018; Sylla et al., 2016; Turp et al., 2014) over the last two decades. The regional climate simulations in this study are conducted using the version 4.4 of RegCM which is a hydrostatic regional climate model developed by the ICTP (Giorgi et al., 2012; Pal et al., 2007). Projected changes in mean temperature and precipitation climatology during the periods of 2010–2040 (near-term), 2040–2070 (mid-term), and 2070–2100 (long-term) with respect to the reference period of 1970–2000 are investigated for the CORDEX-MENA domain using regional climate model simulations. According to many recent studies, there is no common best convective parameterization scheme within RegCM4 for the simulation of both temperature and precipitation (e.g. Almazroui, 2016; Almazroui et al., 2015) due to different climatic characteristics of this domain. Almazroui (2016) also claims that BATS (Biosphere and Atmosphere Transfer Scheme) (Dickinson et al., 1993) performs better as the land-surface scheme and Grell (Grell, 1993) with

Table 2
Some statistics for seasonal precipitation (mm/day) weighted over the whole domain and sub domains for the reference periods of 1980–2000 for ERA-Interim, and 1970–2000 for GCMs and RegCM.

Whole domain		ERA	RegCM_ERA	GCM_MPI	RegCM_MPI	GCM_HadGEM2	RegCM_HadGEM2
SON	Bias	0.528	0.274	0.291	0.741	0.046	0.175
	RMSE	1.219	2.935	0.947	3.240	1.034	1.624
	Correlation	−0.128	0.656	0.953	0.716	0.872	0.716
DJF	Bias	0.469	0.218	−0.024	0.163	−0.137	−0.106
	RMSE	1.378	2.689	0.675	1.573	0.654	1.094
	Correlation	−0.263	0.648	0.923	0.744	0.880	0.634
MAM	Bias	0.471	0.421	−0.071	0.363	−0.123	−0.295
	RMSE	1.251	2.731	0.800	1.748	0.934	1.394
	Correlation	−0.164	0.712	0.911	0.823	0.840	0.627
JJA	Bias	0.389	0.534	−0.173	0.765	−0.351	0.123
	RMSE	1.380	2.032	1.016	2.258	1.384	1.729
	Correlation	−0.025	0.833	0.925	0.825	0.859	0.817
Subdomain 1							
SON	Bias	0.002	0.071	0.054	0.218	0.373	0.862
	RMSE	0.118	0.210	0.107	0.337	0.421	1.125
	Correlation	0.184	0.788	0.903	0.736	0.659	0.556
DJF	Bias	0.156	−0.055	−0.511	−0.185	−0.474	−0.110
	RMSE	0.526	0.455	0.613	0.486	0.600	0.486
	Correlation	0.144	0.790	0.792	0.782	0.800	0.757
MAM	Bias	−0.003	0.167	−0.126	0.143	−0.227	0.159
	RMSE	0.200	0.342	0.322	0.315	0.433	0.426
	Correlation	0.293	0.847	0.771	0.865	0.622	0.859
JJA	Bias	−0.063	−0.081	−0.028	−0.039	−0.037	−0.044
	RMSE	0.127	0.151	0.130	0.136	0.122	0.120
	Correlation	0.300	−0.010	0.185	0.150	0.385	0.471
Subdomain 2							
SON	Bias	0.174	−0.070	−0.103	0.106	0.263	0.621
	RMSE	0.291	0.266	0.233	0.246	0.333	0.747
	Correlation	0.934	0.859	0.896	0.926	0.897	0.909
DJF	Bias	0.323	0.096	−0.005	0.355	−0.135	−0.015
	RMSE	0.598	0.714	0.775	1.086	0.419	0.679
	Correlation	0.907	0.778	0.726	0.792	0.847	0.788
MAM	Bias	0.238	0.345	−0.181	0.311	0.536	0.468
	RMSE	0.540	0.620	0.555	0.542	0.921	0.748
	Correlation	0.939	0.905	0.839	0.900	0.854	0.894
JJA	Bias	0.070	−0.007	0.005	0.062	0.162	0.177
	RMSE	0.291	0.269	0.114	0.358	0.359	0.450
	Correlation	0.909	0.862	0.950	0.857	0.891	0.842
Subdomain 3							
SON	Bias	1.667	0.729	0.279	1.034	0.774	0.400
	RMSE	2.129	1.781	0.617	1.865	1.187	2.371
	Correlation	0.586	0.539	0.796	0.568	0.681	0.183
DJF	Bias	0.493	−0.294	−0.347	−0.298	−0.105	−0.260
	RMSE	0.889	0.420	0.468	0.405	0.259	0.404
	Correlation	0.383	0.538	0.819	0.668	0.764	0.516
MAM	Bias	1.042	0.227	−0.229	0.245	0.204	−1.200
	RMSE	1.488	1.351	0.701	1.460	1.012	1.836
	Correlation	0.689	0.572	0.831	0.513	0.574	0.230
JJA	Bias	2.395	2.937	0.000	3.431	0.371	0.371
	RMSE	3.390	4.088	1.275	4.023	1.091	3.186
	Correlation	0.918	0.803	0.834	0.857	0.881	0.704
Subdomain 4							
SON	Bias	−0.044	−0.056	−0.042	−0.010	−0.026	0.032
	RMSE	0.071	0.099	0.077	0.071	0.062	0.085
	Correlation	−0.900	0.801	0.779	0.794	0.839	0.662

(continued on next page)

Table 2 (*continued*)

Subdomain 4							
DJF	Bias	−0.082	−0.087	−0.123	−0.083	−0.093	−0.075
	RMSE	0.189	0.230	0.247	0.236	0.204	0.219
	Correlation	−0.916	0.874	0.797	0.873	0.882	0.873
MAM	Bias	−0.055	−0.064	−0.076	−0.031	−0.035	−0.015
	RMSE	0.101	0.109	0.109	0.090	0.086	0.082
	Correlation	−0.836	0.359	0.563	0.446	0.542	0.511
JJA	Bias	−0.064	−0.063	−0.063	−0.053	−0.060	−0.021
	RMSE	0.093	0.091	0.091	0.088	0.092	0.072
	Correlation	−0.638	0.307	−0.123	−0.257	−0.329	0.070
Subdomain 5							
SON	Bias	2.707	7.075	2.607	7.758	1.491	−0.694
	RMSE	3.078	11.329	2.841	8.888	2.188	2.194
	Correlation	0.042	0.011	0.136	−0.212	−0.635	0.235
DJF	Bias	3.814	2.988	−0.019	−0.307	−1.515	−3.075
	RMSE	4.104	6.628	1.042	1.883	1.773	3.241
	Correlation	0.726	0.750	0.928	0.498	0.766	0.711
MAM	Bias	2.564	6.546	0.452	2.987	−0.800	−3.023
	RMSE	2.928	8.865	0.944	4.210	0.908	3.164
	Correlation	−0.024	−0.157	0.584	0.038	0.374	0.364
JJA	Bias	1.463	3.333	−0.926	3.320	0.033	−0.785
	RMSE	1.696	3.759	1.073	4.098	0.708	1.031
	Correlation	0.892	−0.330	0.939	0.538	0.896	0.802

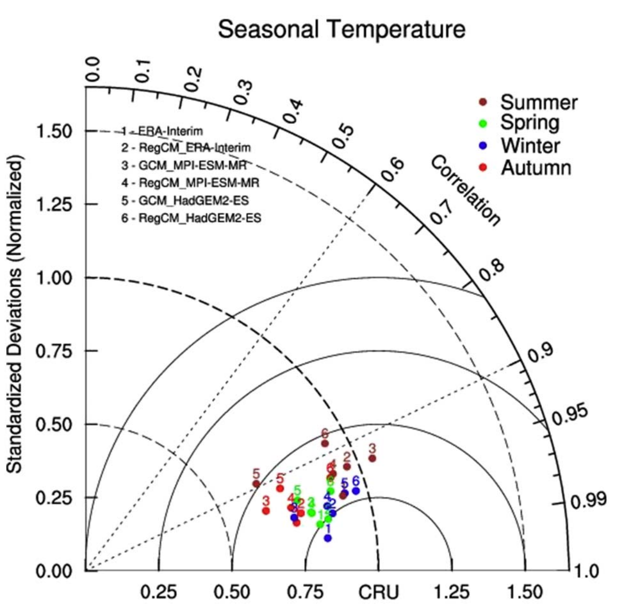

Fig. 5. Taylor diagram for the simulated temperature data obtained from RegCM4.4, GCM and ERA-interim simulations with respect to CRU dataset.

the Fritsch-Chappell type closure (Fritsch and Chappell, 1980) as the most appropriate option for convection scheme in the model. In all of the simulations in this study these land-surface and convection schemes are employed.

MENA region is defined as a domain with the corner points at 27.00° W – 45.00° N, 76.00° E – 45.00° N, 27.00° W – 7.00° S, and 76.00° E – 7.00° S within the CORDEX framework. The outputs of two global circulation models (i.e. HadGEM2-ES of the Met Office Hadley Centre, MPI-ESM-MR of the Max Planck Institute for Meteorology) (Taylor et al., 2012) are dynamically downscaled to 50 km resolution under both RCP4.5 and RCP8.5 emission scenarios (Van Vuuren et al., 2011). HadGEM2-ES and MPI-ESM-MR are used as driving fields because their performance is relatively better than other global climate models for this domain as is already discussed in the literature (Endris et al., 2015).

The comparison between model results and the CRU observational data are also made by calculating some basic inferential statistics consisting of bias, Root Mean Square Error (RMSE) and Pearson's correlation coefficient for five distinct subdomains and the whole domain. All datasets are gridded to $0.5 \times 0.5^{\circ}$ resolution using bilinear interpolation method, in order to treat the different size and different number of grid-boxes originating from the different horizontal resolution of the CRU, ERA-Interim, GCM, and RegCM datasets.

3. Results

3.1. Model biases in seasonal temperature and precipitation climatology

In the present work, the regional climate model's performance in simulating observed climate of the region is first investigated by using ERA-Interim reanalysis dataset and global climate hindcast models of HadGEM2-ES and MPI-ESM-MR as a forcing data to the model. For this purpose, we run the regional climate model with ERA-Interim reanalysis dataset for the period of 1980–2000 and global climate models of HadGEM2-ES and MPI-ESM-MR for the period of 1970–2000 to investigate model biases for four seasons, which are taken as December–January–February (DJF, winter), March–April–May (MAM, spring), June–July–August (JJA, summer) and September–October–November (SON, autumn). Even though parts of this region are within the tropics we give the main emphasis on the Middle East/North Africa part where these are the four seasons generally observed. Model's skill in simulating observed climatology is spatially and temporally evaluated by comparing the output of regional climate model with the CRU observational dataset for seasonal temperature and precipitation values. A comparison of biases with respect to CRU data in surface temperature for the RegCM4.4 forced by different global datasets for seasonal temperature is presented in Fig. 1. A cold bias of about 2 °C can be

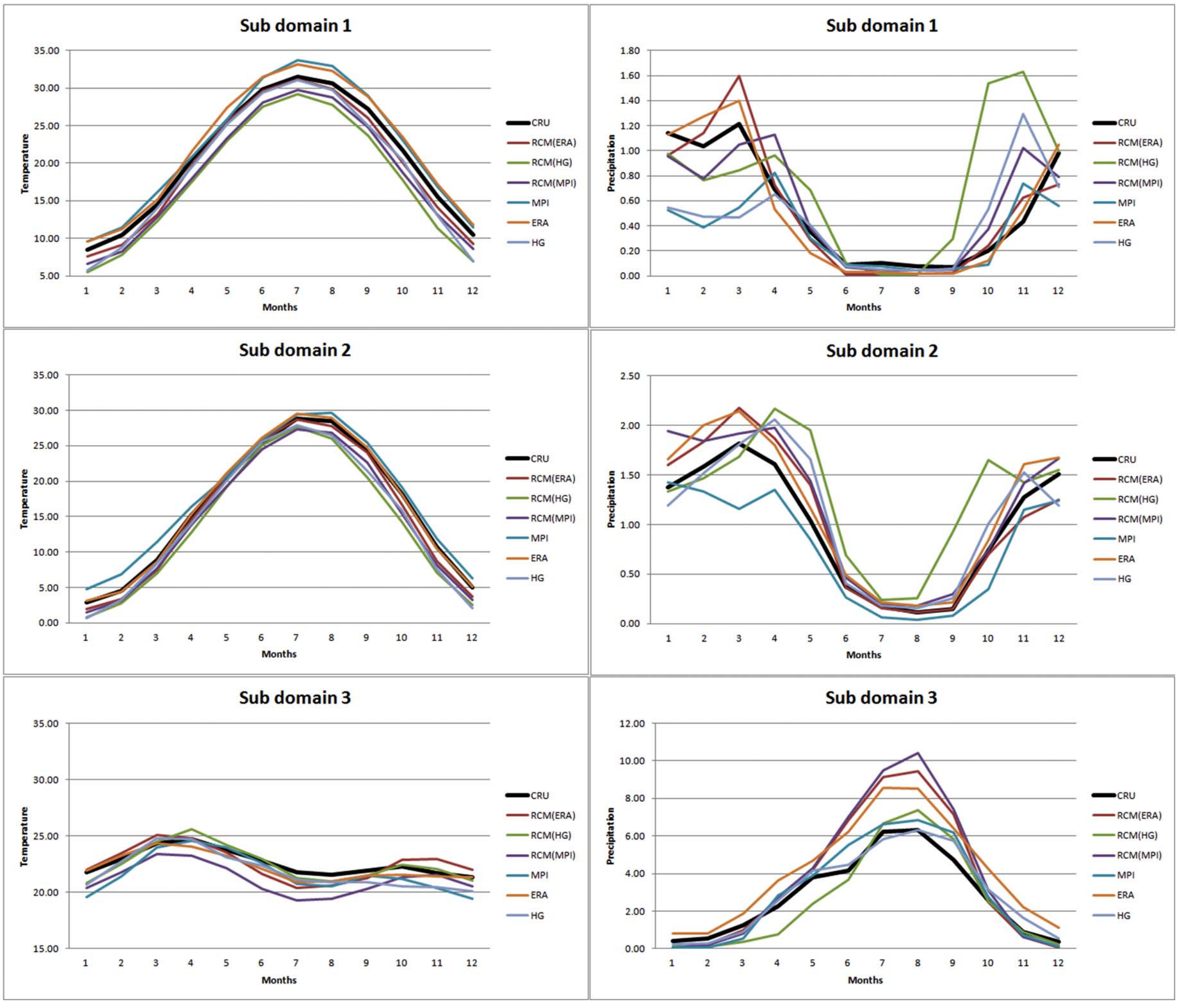

Fig. 6. Annual cycles of air temperature (°C) and precipitation (mm/day) of subdomain 1–3.

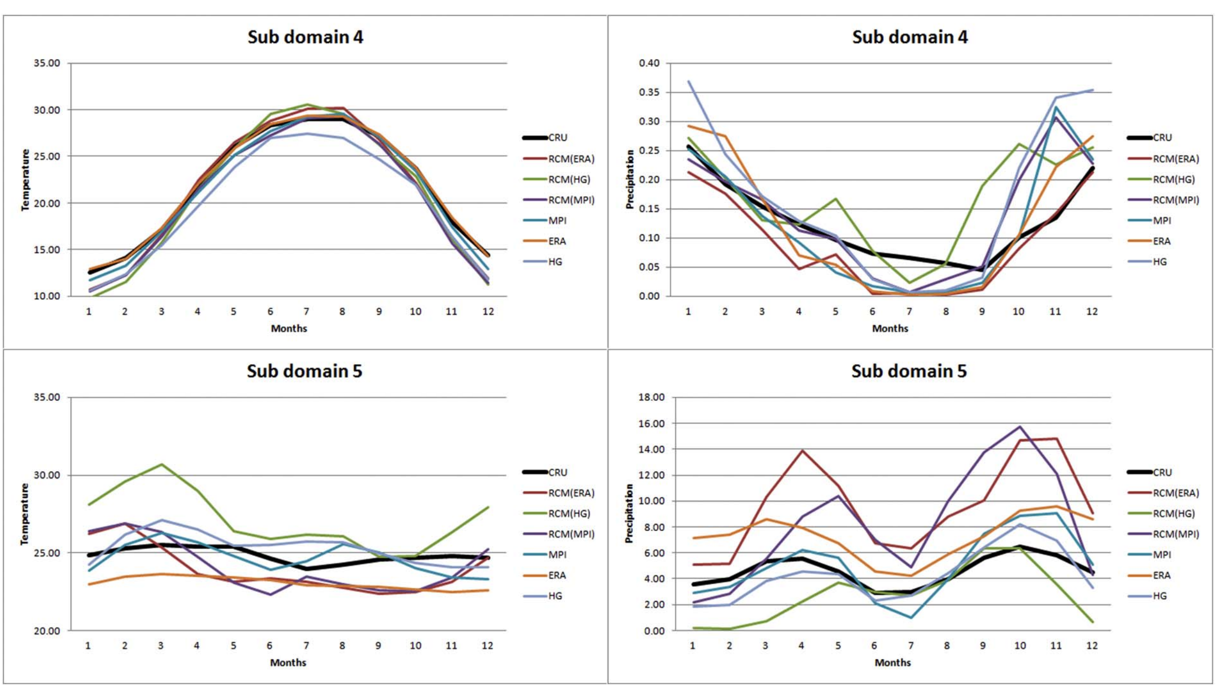

Fig. 7. Annual cycles of air temperature (°C) and precipitation (mm/day) of subdomain 4 and 5.

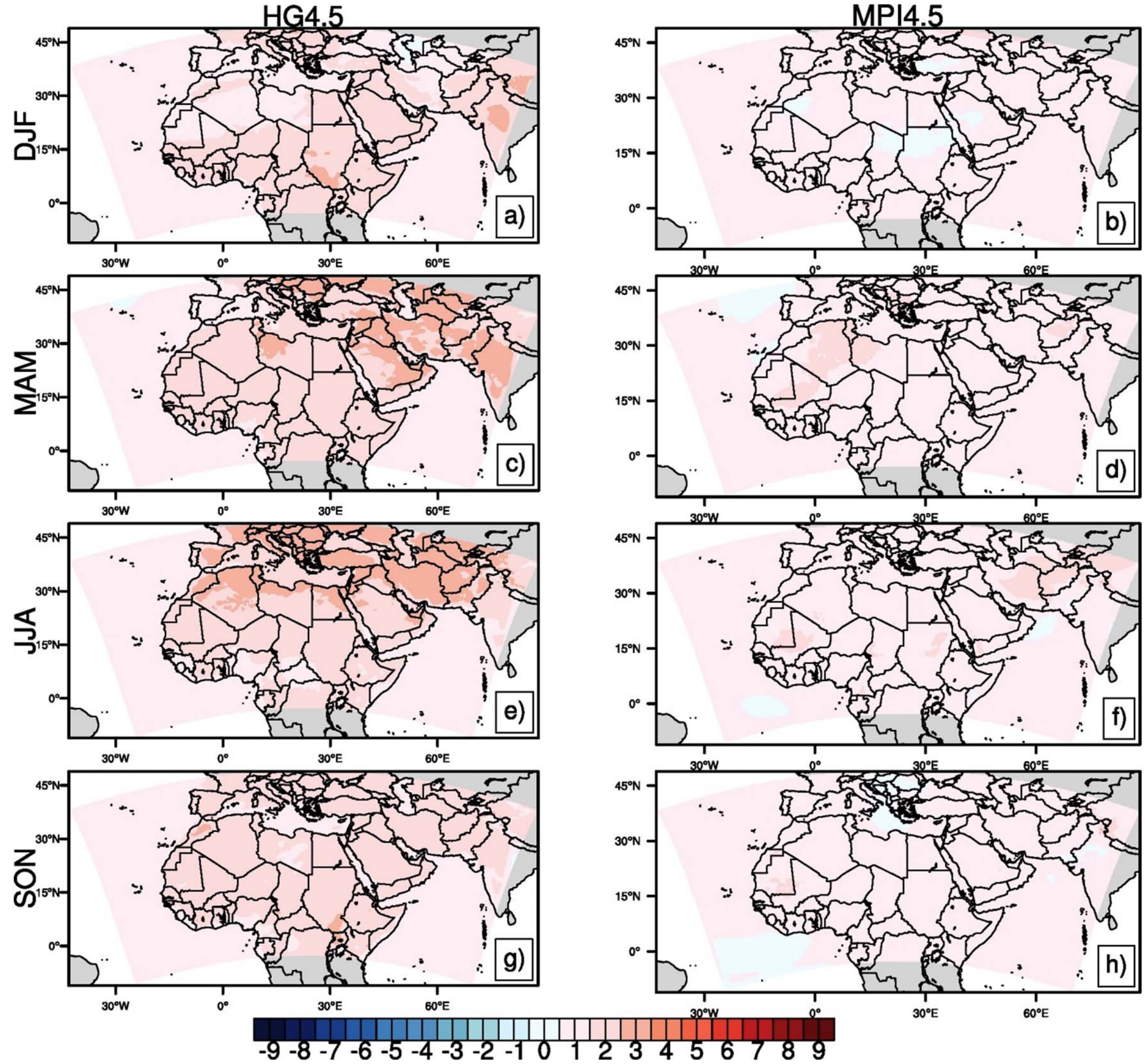

Fig. 8. Changes in projected mean temperatures (°C) obtained for RegCM4.4 simulations with HadGEM2-ES (RCP4.5) for the period of 2010–2040 with respect to period of 1970–2000: (a) winter, (c) spring, (e) summer and (g) autumn seasons. Same results but with the MPI-ESM-MR dataset are: (b) winter, (d) spring, (f) summer and (h) autumn seasons.

observed in the central part of the domain in RegCM simulation driven by ERA-interim as compared to observational dataset in winter. This cold bias is absent in other three seasons (Fig. 1b, c, d). This cold bias in winter can also be seen in RegCM simulation driven by HadGEM2-ES dataset. HadGEM2-ES global dataset has also stronger cold bias itself for winter season especially over the North Africa and Arabian Peninsula. Therefore, this cold bias is inherited by global climate models. On the other hand, cold biases, especially in the Sahel-Sahara region, can be attributed to use of the RegCM4.4 without mineral dust module in this study (Ji et al., 2016b; Zittis and Hadjinicolaou, 2017). However, warm bias over the arid Arabian Peninsula (over Oman) mentioned by Almazroui et al. (2016) is observed during summer season in outputs of the model driven by different global datasets. According to Almazroui et al. (2016), warm bias over Oman is inherited by global datasets. The reason for this bias can be the representation of incorrect soil type values in these global datasets (Almazroui et al., 2016). RegCM outputs driven by MPI-ESM-MR show better agreement than the results of RegCM driven by HadGEM2-ES global model with respect to the observational dataset. Nevertheless, an overall bias of the output is roughly between −3.0 and 3.0 °C for temperature.

The RegCM4.4 also overestimated air temperatures over mountainous and high plateau regions of the domain including the Himalayas, eastern portion of Turkey, the Iran Plateau and Plateau of Tibet, regardless of seasons and the boundary conditions used. This result can be explained by inadequate observational data due to lack of climatological and meteorological stations in those regions of the domain. As this cold bias is mainly observed around mountainous parts of the region, this might be a result of the station data bias, because the meteorological/climatological stations are mostly located in the valleys and relatively lower geomorphological landscape types of this region. This situation may have resulted in higher representative temperature readings for the region. Station based temperature observations are likely to be overestimated for various reasons, including a low elevation station bias (especially over the high mountainous area) and sparse network of stations (Ozturk et al., 2017).

In Fig. 2, a comparison of biases with respect to CRU observational dataset in precipitation data for the RegCM4.4 forced by different global datasets and CRU data for seasonal precipitation are presented. Results show that regional climate model overestimates precipitation over southern part of the domain which has wetter condition, especially

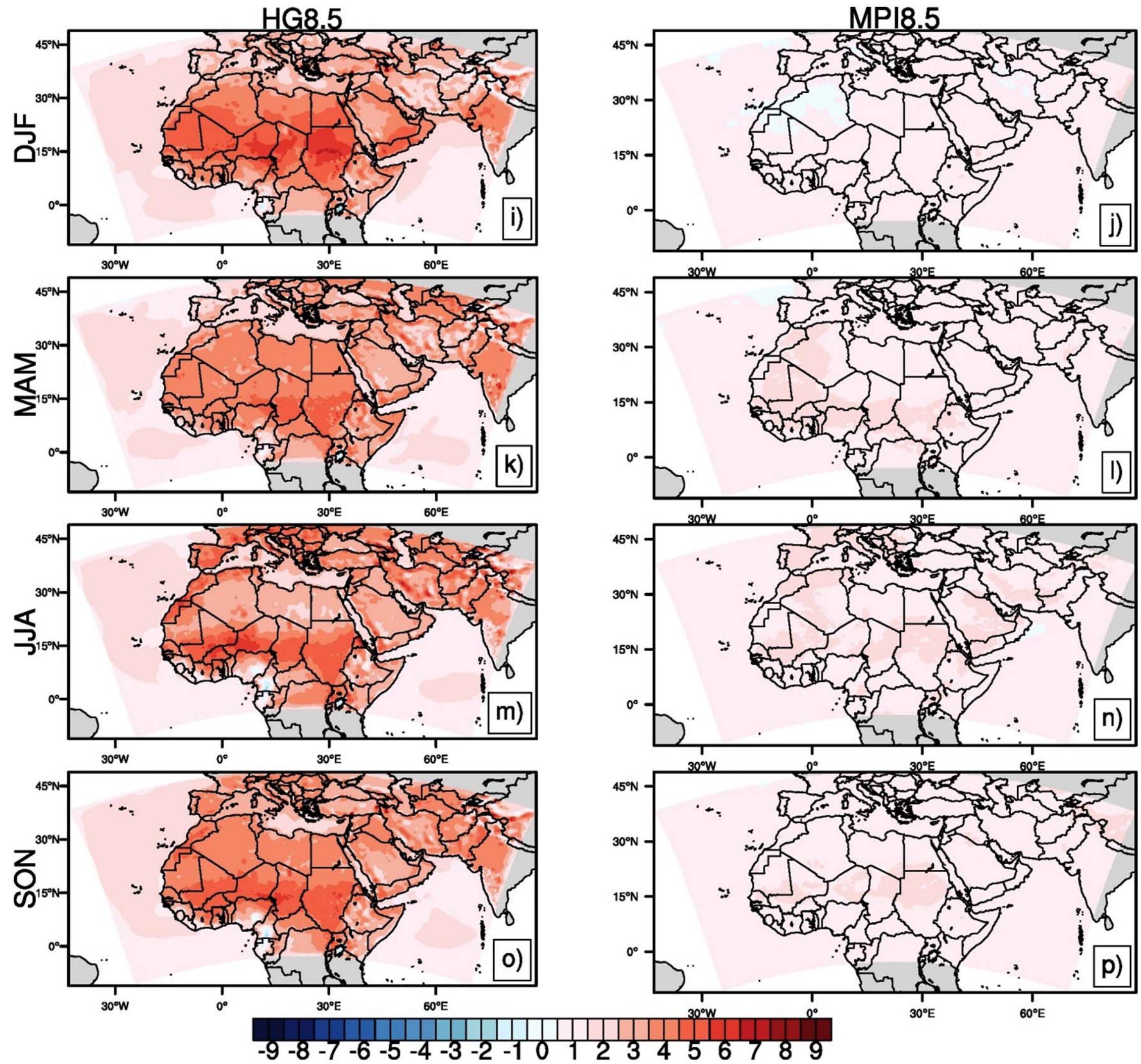

Fig. 9. Changes in projected mean temperatures (°C) obtained for RegCM4.4 simulations with HadGEM2-ES (RCP8.5) for the period of 2010–2040 with respect to period of 1970–2000: (a) winter, (c) spring, (e) summer and (g) autumn seasons. Same results but with the MPI-ESM-MR dataset are: (b) winter, (d) spring, (f) summer and (h) autumn seasons.

for summer seasons. The Grell scheme (Grell, 1993) with the Fritsch-Chappell type closure that is used in model is probably the best single option among all the convective scheme options for precipitation for the entire region. The reason for wet bias can be the fact that RegCM oversimulates air pressure and water vapor values along with lower wind speeds compared to driving datasets (Almazroui et al., 2015). There is not much difference in output of regional model run by different global datasets. Model output agrees with observation over the Great Sahara Desert, the Western Sahara and the Sahel biogeographical regions, which have already arid/hyper-arid, arid/semi-arid and arid/semi-arid climates, respectively.

The annual average pattern of bias values for temperature and precipitation is presented in Fig. 3. Cold bias is still observed around mountainous parts of the region according to annual averages of regional climate model's output. Performance of regional climate model in reproducing annual precipitation values is reasonable (Fig. 3d, e, f).

The comparisons, which include some basic inferential statistics (i.e. bias, Root Mean Square Error (RMSE), correlation coefficient), are also made for five distinct subdomains (Fig. 4) as well as the whole domain. Subdomains were selected considering the genetic global climate patterns as defined in the Köppen-Geiger classification (Peel et al., 2007). In general, the MENA region generally has six major climatic types including (i) equatorial and tropical humid climates, (ii) wet summer tropical monsoon climate (the West Africa and southwest Asia monsoon climates), (iii) wet summer tropical and subtropical semi-humid and semiarid climates, (iv) arid and hyper-arid desert climates, (v) dry summer subtropical Mediterranean climate, and (vi) humid and semi-humid temperate (mid-latitude) climates with mild winters. Broadly subdomain 1 (Iran), subdomain 2 (the north-midwestern part of the Arabian Peninsula) and subdomain 4 (Egypt) represent arid regions, whereas the other subdomains (ie. subdomain 3 - Ethiopia and subdomain 5 - DR Congo -) represent semi-humid and humid regions. Since each climatic type consists of various sub-climate types depending on boundary condition dataset and regional physical geographical characteristics such as topography, elevation and exposure, land-sea distribution, continentality and latitude factors, these five subdomains also differ from each other. Temperature and precipitation statistics obtained from spatial averages for subdomains are presented in Tables 1 and 2. The Pearson correlation coefficients for long-term seasonal means (i.e. SON, DJF, MAM, and JJA) are calculated spatially.

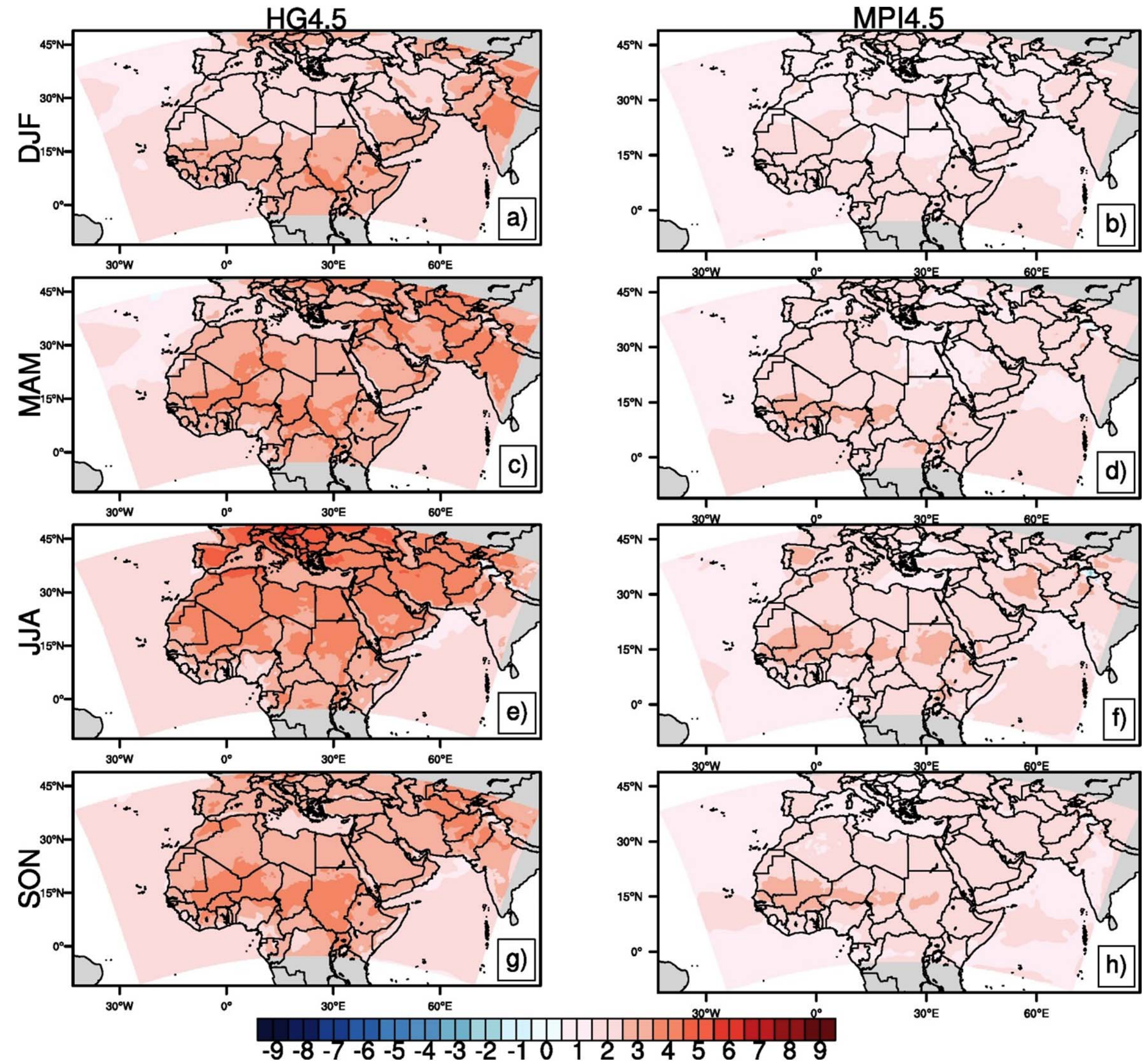

Fig. 10. Same as Fig. 8, but for the period of 2040–2070 with respect to the period of 1970–2000.

Additionally, Taylor diagram showing standardized deviations and correlation coefficients for temperature is also presented in Fig. 5. Although RegCM causes a cold bias over the MENA region, it is very successful in capturing spatial pattern of seasonal mean temperature for all seasons as shown in the Fig. 5.

When the statistical metrics given in Table 1 are examined, it is seen that all model and reanalysis outputs are highly correlated with land-based observational values. Moreover, simulations using RegCM result in cold bias. The bias is higher in winter than in summer. ERA-Interim and MPI-ESM-MR simulations have the lowest bias originally. The notable point here is that HadGEM2-ES global model already has cold bias over the MENA region for all seasons.

Since the entire domain is a vast area, consequently the model biases can vary in a large scale. For instance, over the subdomain 1, the biases are the highest for all seasons. Both of MPI-ESM-MR and HadGEM2-ES driven results show that RegCM causes larger cold biases, over Iran with high topography and dry climate than the whole domain. Similarly, RegCM increases the cold bias over subdomain 2, where dry-summer subtropical Mediterranean climate is observed. RegCM performs fairly well in subdomain 3. It dramatically improves the cold bias of ERA-Interim and HadGEM2-ES for autumn and spring seasons. In low-latitude deserts (i.e. subdomain 4), RegCM enhances the temperature bias except for MPI-ESM-MR in summer and HadGEM2-ES in spring. ERA-Interim in the subdomain 5 is less correlated with CRU than in other domains and it has the highest bias values. In contrast, RegCM reduces the bias of ERA-Interim in the subdomain 5, climate of which is moist tropical. Therefore, it can be said that RegCM simulates lower temperature than the driving fields (Almazroui et al., 2016).

In the case of precipitation, as shown in the Table 2, RegCM overestimates the precipitation except for HadGEM2-ES in winter and spring. However, when we compare the results of ERA-Interim with the results of downscaled ERA-Interim, it is concluded that the negative correlation coefficients of ERA-Interim with respect to the CRU become the positive for all seasons. However, both cases (coarse and high resolutions) of HadGEM2-ES give underestimated results for the entire domain in winter and spring. The correlations between the simulations and CRU are much better for the subdomains 2 and 4. By contrast, RegCM improves the biases in some cases. For example, for winter season in subdomain 1 MPI-ESM-MR and HadGEM2-ES biases are slightly reduced by RegCM. Similarly, in subdomain 2 bias of the downscaled HadGEM2-ES for spring season is lower than bias of the original HadGEM2-ES. Besides, in subdomain 4 biases, except

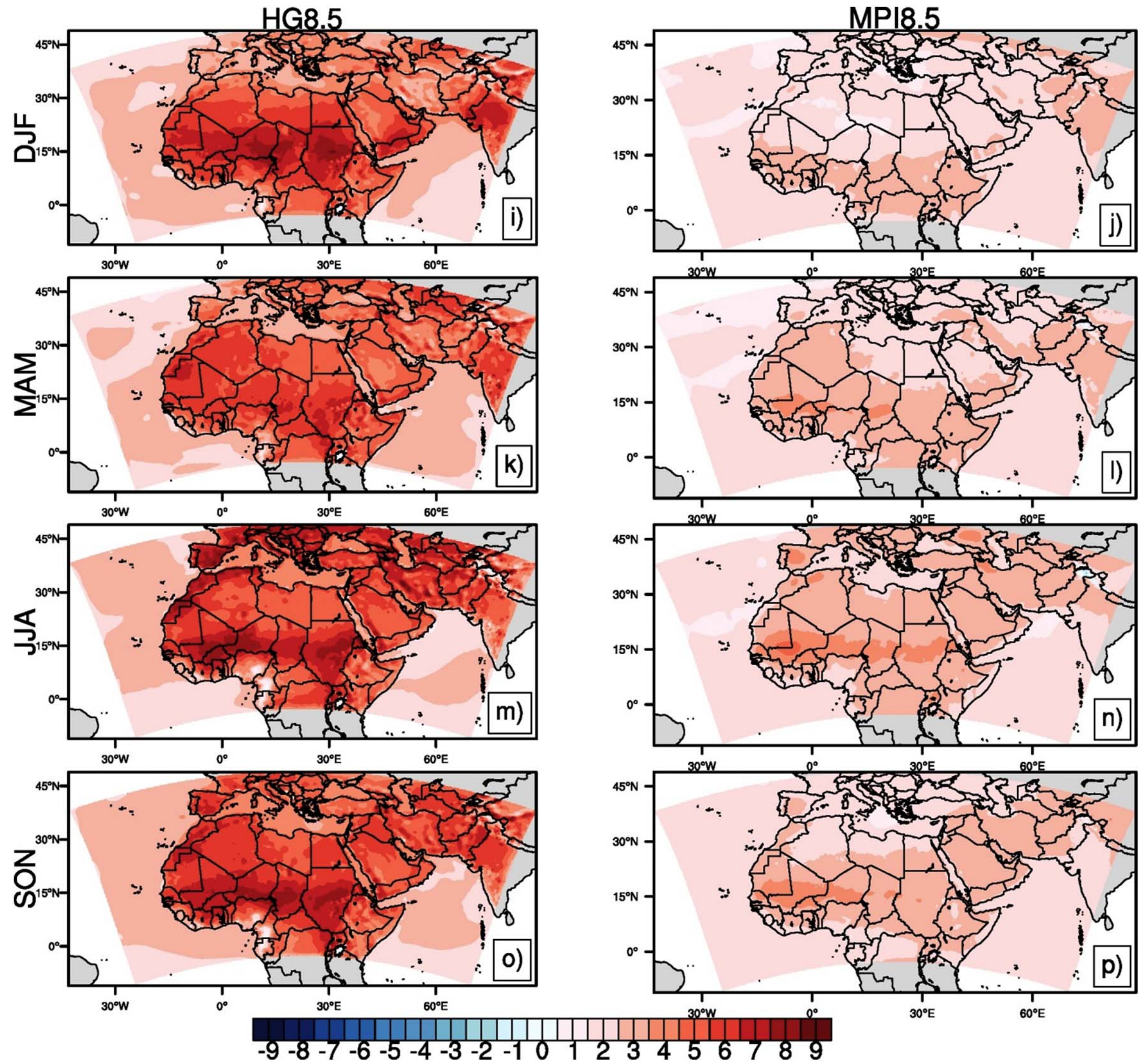

Fig. 11. Same as Fig. 9, but for the period of 2040–2070 with respect to the period of 1970–2000.

HadGEM2-ES for autumn, are improved by the RegCM.

Annual cycles of temperature and precipitation of selected subdomains are presented in Figs. 6 and 7. According to the results, RegCM has simulated annual cycles of temperature well for dry regions (i.e. subdomain 1, 2, and 4). Even though the amounts of precipitation during the year for dry regions are not reproduced well by model, seasonal trends are captured reasonably. The precipitation for dry regions is overestimated compared to driving fields especially for cold seasons. The model does not capture annual cycle of both temperature and precipitation well for wet region (i.e. subdomain 5). RegCM also overestimates precipitation for tropical region. On the other hand, annual cycle of both variable for subdomain 3 (i.e. Ethiopia) which has humid climatic characteristics is reproduced well by RegCM except overestimation of precipitation. Reason for this result can be highland characteristics of that region. It has mild temperate climatic conditions (Peel et al., 2007; Türkeş, 2017).

Eventually, evaluation part of the study reveals that RegCM has good agreement with observation for the temperature climatology but the performance of the model is less reliable for the precipitation climatology. RegCM's ability to capture the temperature and precipitation climatology over the MENA region varies spatially and temporally. Therefore, the model's performance appears more satisfactory for arid climatic zones than that of humid regions. The main purpose of CORDEX regions is to provide a framework in which different groups perform simulation runs in the exact same domain. However as some of these domains may well be “more politically” determined rather than scientifically, we observe the results we have obtained. All of these runs were performed using latest version of RegCM, RegCM4.4 at the time of the runs and single parametrization schemes were used for the whole domain. Future runs will be performed using newer versions of RegCM where different parametrization schemes will be used for different subdomains.

3.2. Projected changes in future temperature and precipitation climatology

3.2.1. Changes in air temperature

The temperature outputs of regional model run by two different global models for the period of 2010–2040, 2040–2070, and 2070–2100 with respect to present period based on the RCP4.5 and RCP8.5 emission scenarios are presented in Figs. 8–13. The 95-percentile confidence ranges of change signal for the period of 2070–2100 with respect to period of 1970–2000 are also given in Figs. 12 and 13.

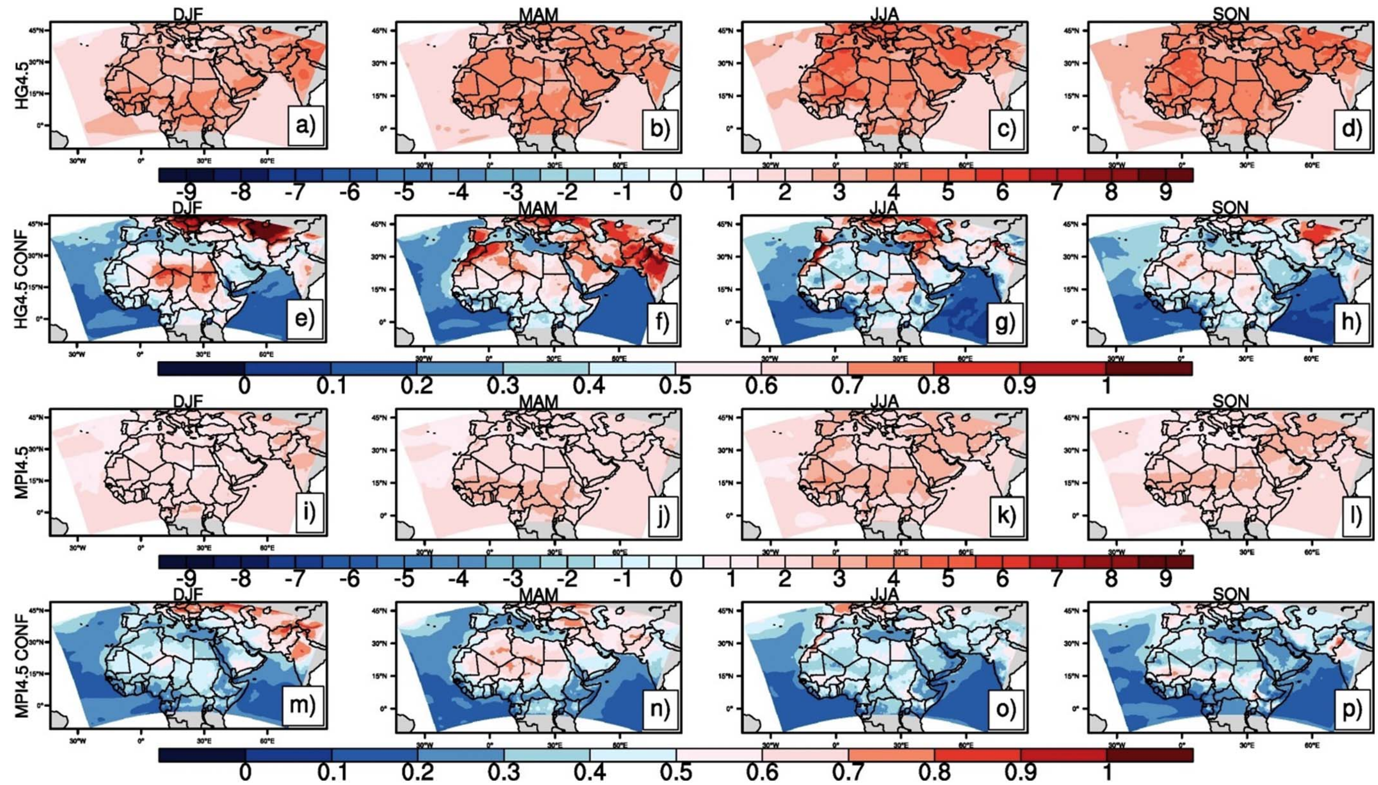

Fig. 12. Changes in projected mean temperatures (°C) obtained for RegCM4.4 simulations with HadGEM2-ES (RCP4.5) for the period of 2070–2100 with respect to the period of 1970–2000 and the 95 percentile confidence ranges: (a, e) winter, (b, f) spring, (c, g) summer and (d, h) autumn seasons, respectively. Same results but with the MPI-ESM-MR dataset are: (i, m) winter, (j, n) spring, (k, o) summer and (l, p) autumn seasons.

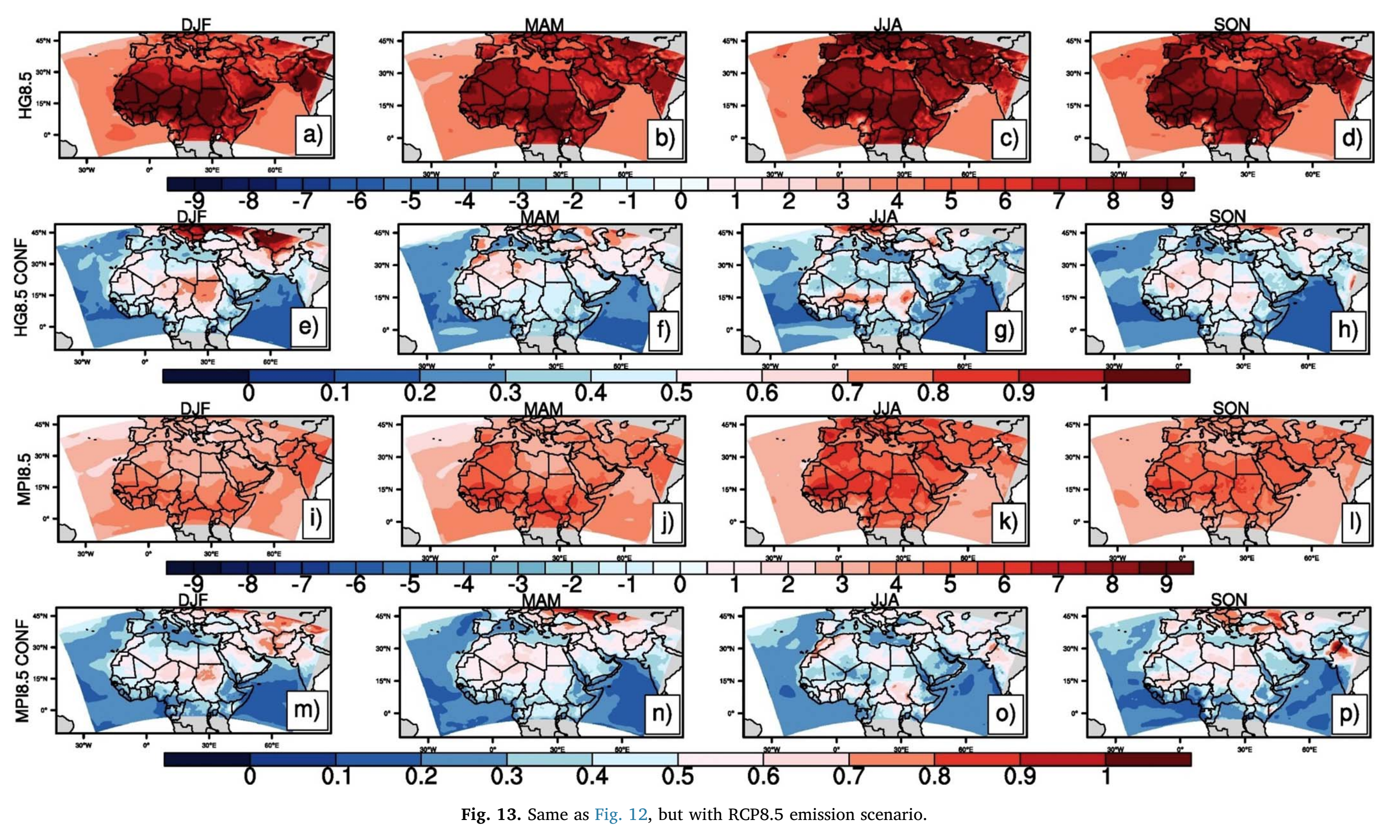

Fig. 13. Same as Fig. 12, but with RCP8.5 emission scenario.

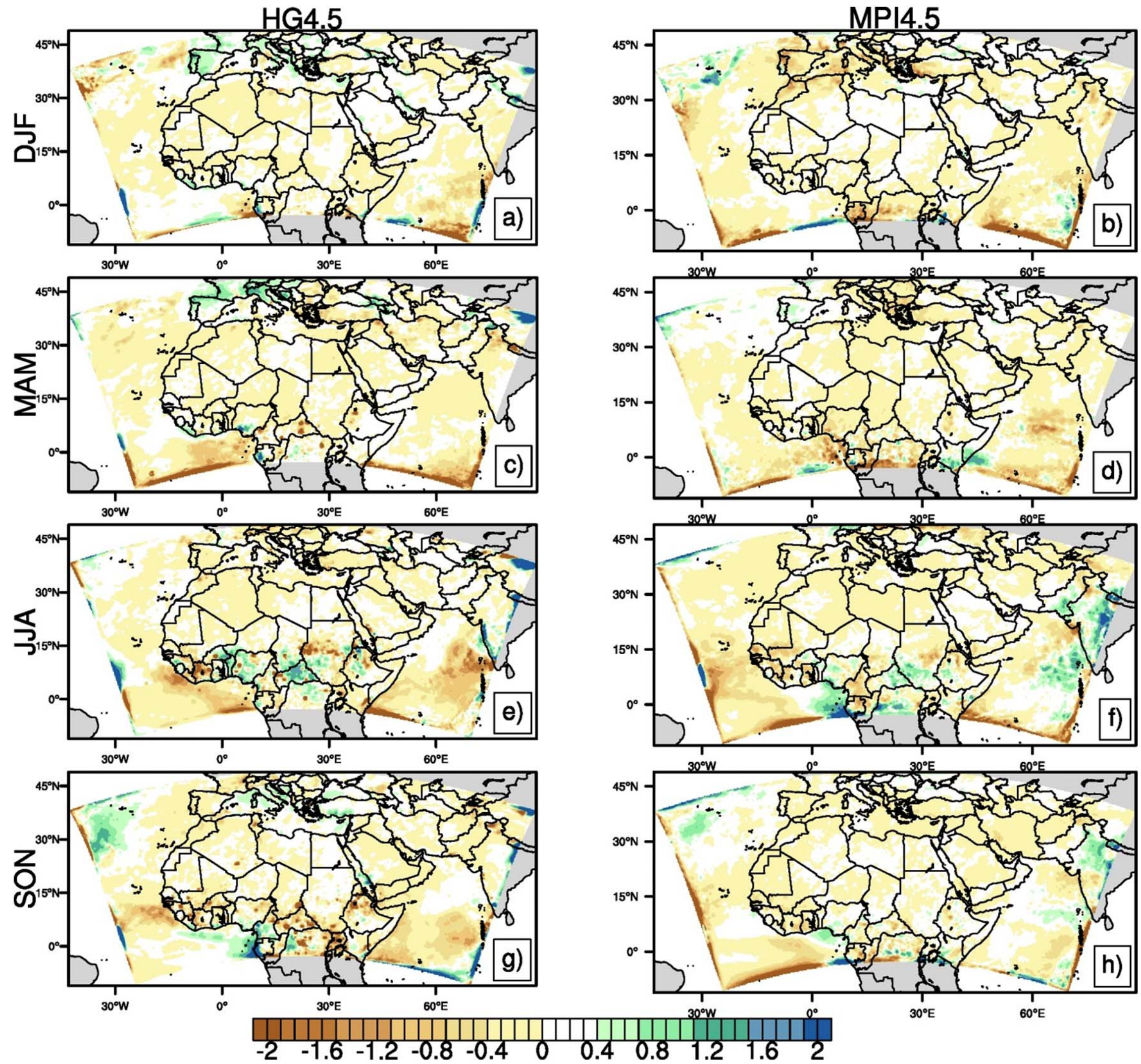

Fig. 14. Changes in projected total precipitation amounts (mm/day) obtained for RegCM4.4 simulations with HadGEM2-ES (RCP4.5) for the period of 2010–2040 with respect to period of 1970–2000: (a) winter, (c) spring, (e) summer and (g) autumn seasons, respectively. Same results but with the MPI-ESM-MR dataset are: (b) winter, (d) spring, (f) summer and (h) autumn seasons.

According to the modeling results, the output of MPI-ESM-MR global model dataset show similar trend with the global model of HadGEM2-ES. However, the magnitude of warming projected by HadGEM2-ES global model is more than that of MPI-ESM-MR global model projections especially in RCP8.5 emission scenario for the period of 2070–2100 (Fig. 12). According to HadGEM2-ES based simulation results in RCP8.5 scenario case, scorching temperatures will dominate significantly over the Sahel zone, the Atlas Mountains, and the Iberian Peninsula, especially in the summer season. For the entire domain, general warming trend is projected by regional model for all three future periods with respect to the present climatology. Projected warming is increasing with time and most of the warming will be during the 2070–2100 period. Also, the 95 percentile confidence range values change between 0 and 0.8 °C for all of the domain except for the northern Balkan region (Figs. 12 and 13). Results of this uncertainty for temperature change signal indicate that all changes can be considered robust. In the northern Balkan region, uncertainty range is increasing to 17%, which is also consistent with results of Lelieveld et al. (2014).

Results based on RCP4.5 model scenario show that the temperature for summer season will increase by 4–5 °C for all of the region for the period of 2070–2100. According to RCP8.5 model scenario results the temperature increase will be more than 9 °C for almost all parts of the domain and for all seasons. In the MENA region, the increase in temperatures over the Mediterranean Basin, Southern Europe and western Turkey for winter season will be the lowest according to future projections. In general, the regional simulation results for temperature are nearly consistent with the results presented in the atlas of global and regional climate projections produced in AR5. In AR5, it is expected that the temperature changes over this region will be gradually towards warmer temperatures as time passes (IPCC, 2013b). Moreover, in the report it is obvious that these changes will become more intense for RCP8.5 scenario as compared to RCP4.5 (IPCC, 2013b). For instance, when the outcomes of twenty-year mean changes over the South Europe/Mediterranean domain, are examined, CMIP5 multi-model ensemble results show that the long term (2081–2100) winter mean temperature will be 1 to 3 °C higher than the average of 1986–2005 for

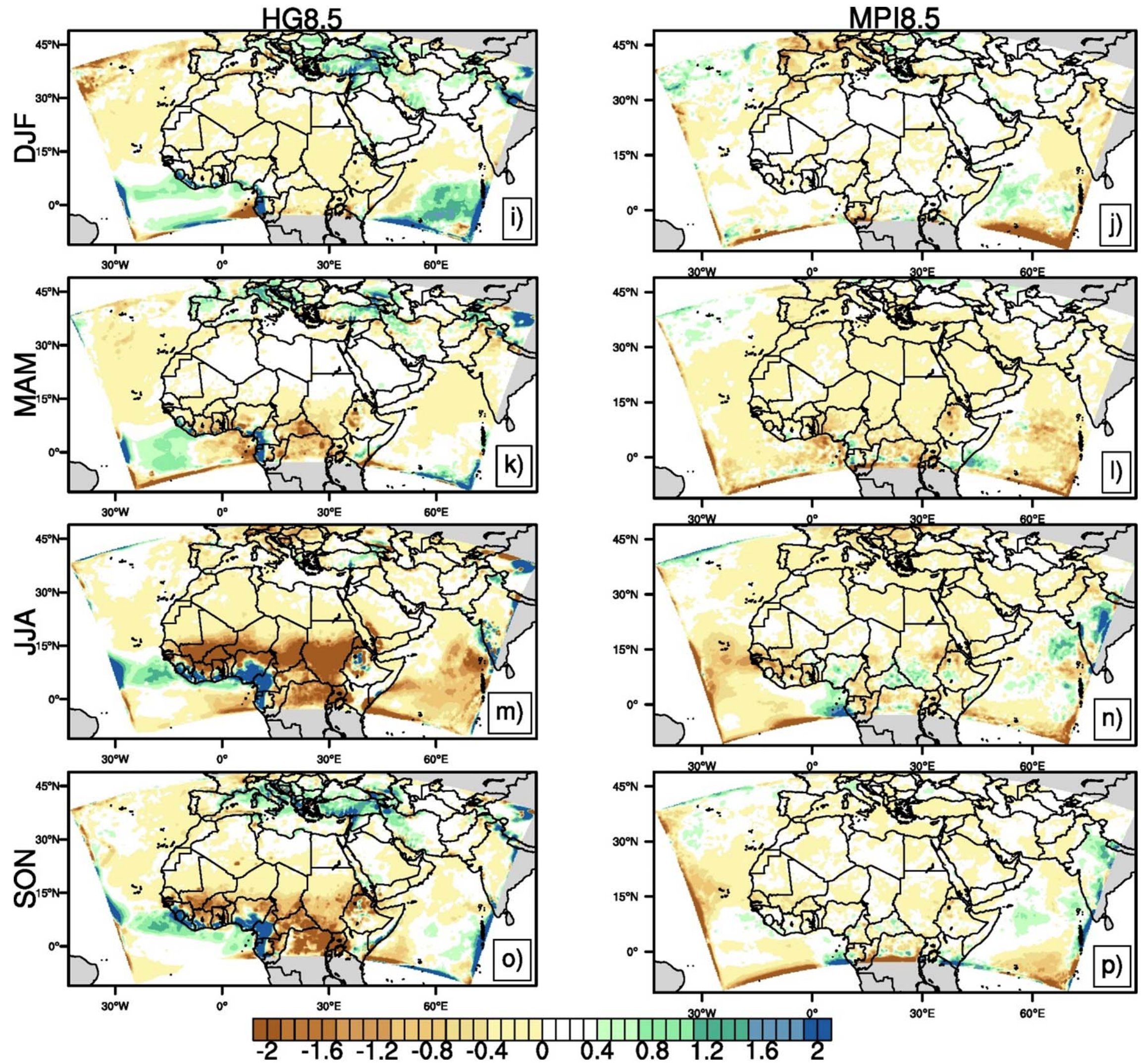

Fig. 15. Same as Fig. 14, but for RCP8.5 scenario.

RCP4.5. The same will be 3 to 7 °C higher with regard to RCP8.5 (IPCC, 2013b). Summer temperature increases will also reach up to 4 °C and 9 °C for RCP4.5 and RCP8.5 cases, respectively (IPCC, 2013b).

3.2.2. Changes in precipitation

The change in precipitation for the future periods of 2010–2040, 2040–2070 and 2070–2100 with respect to the present period of 1970–2000 based on the IPCC's RCP4.5 and RCP8.5 emission scenarios are presented in Figs. 14–20. The 95-percentile confidence ranges of change signal for the period of 2070–2100 with respect to period of 1970–2000 are also given in Fig. 20. According to the model results, there is no marked change in the amount of precipitation in the Great Sahara Desert, the Sahel zone and the Northern Africa, which are characterized mostly with hyper arid/arid, arid/semiarid, and semi-arid/dry-sub humid climatic and physical geographic conditions (Türkeş, 2017), respectively. Results of RegCM4.4 driven by HadGEM2-ES global model of RCP8.5 scenario output show much increase in precipitation with respect to present period for the spring season, even though it is much less in value. This is the result of hyper arid/arid climatic and physical geographic conditions of the aforementioned region. During the summer and autumn seasons, amounts of precipitation in the southern part of the domain whose climate is controlled by the West African monsoon system decrease severely for all future periods with respect to the hindcast period of 1970–2000.

Drier conditions are simulated by the models for the most part of the region, which is already arid and semi-arid. Both emission scenarios' output shows similar results for future projections. There will be a decrease in precipitation amounts in the Greater Mediterranean region especially in southern Europe for the summer season and for the winter season except for Turkey. For the winter season, the output of HadGEM2-ES global model shows increase in precipitation, whereas MPI-ESM-MR global datasets projects decrease in precipitation for Turkey and its surrounding region. Results based on RCP8.5 emission scenario output show more severe decrease in precipitation, especially in the southern part of the domain. In addition, it is remarkable that an increase in summer and autumn precipitation amounts throughout the Gulf of Guinea is predicted by the HadGEM2-ES global model based simulation for RCP8.5 scenario case. In the AR5, when the atlas of global and regional climate projections are examined, it can be concluded that the most parts of the South Europe/Mediterranean domain experience a decrease in average precipitation (IPCC, 2013b). Decrease in precipitation will be significant over the southern-southwestern parts

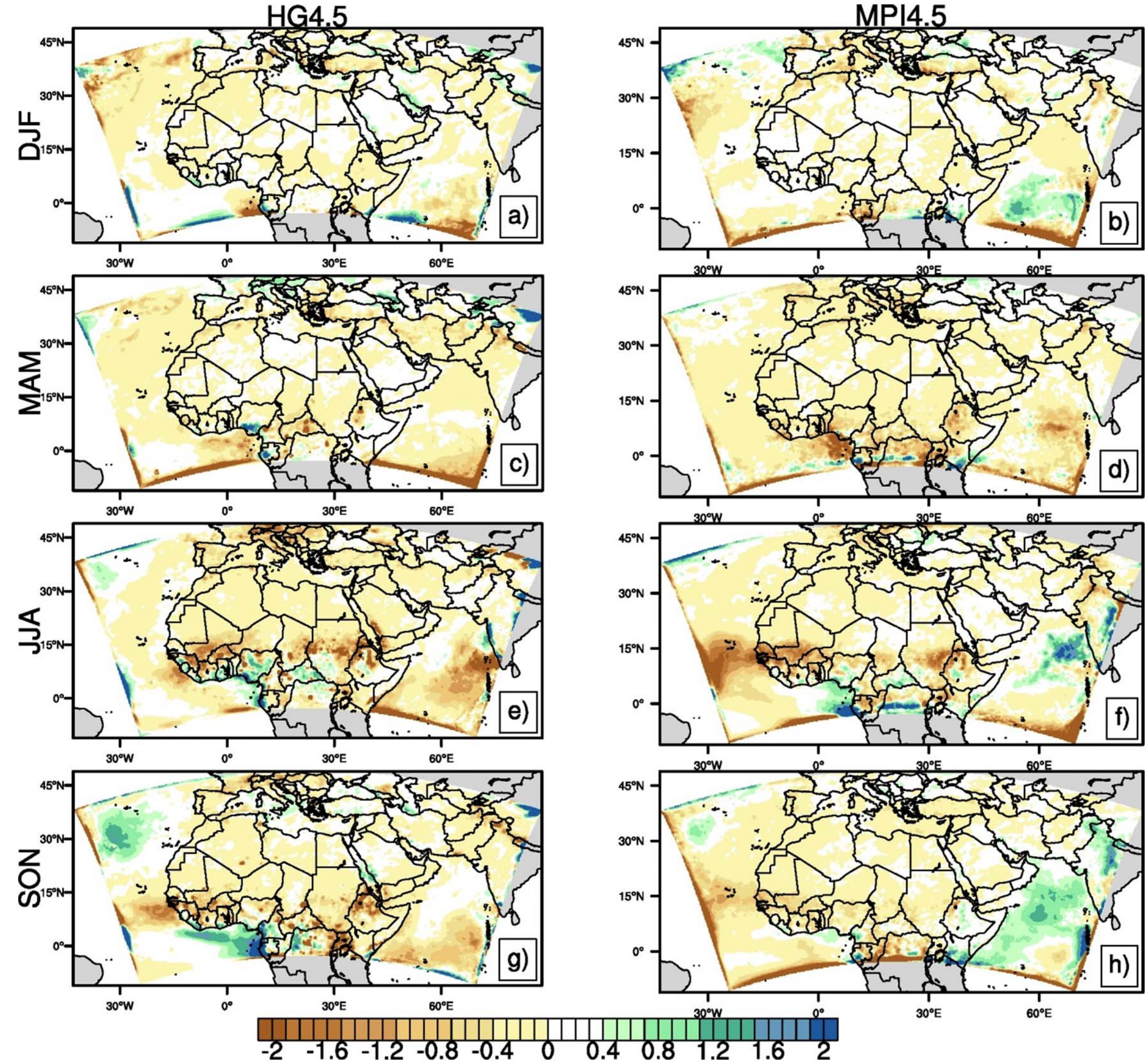

Fig. 16. Same as Fig. 14 but for the period of 2040–2070.

of Turkey and Cyprus in the winter season for the period of 2081–2100 with respect to the period of 1986–2005 (IPCC, 2013b). Severity of the decrease in precipitation is more pronounced for the RCP8.5 scenario with respect to RCP4.5 scenario (IPCC, 2013b). Analysis of the same periods for the autumn season shows that decrease in precipitation will spread on a large area but an increase will be explicitly observed throughout the Sahel region and the Arab domain (IPCC, 2013b), possibly related to the northward shift of the ITCZ. Unlike temperature simulations, in the RegCM simulations of precipitation, the regional modeling results do not coincide with the AR5 atlas results. For instance, the increase in precipitation for autumn season over the Sahel region and the Arab domain is presented much well by MPI-ESM-MR driven simulation.

Additionally, the 95 percentile confidence range values for precipitation change between 0 and 0.1 mm/day almost in all parts of the domain except for the southern part, which has wetter condition especially for summer seasons (Fig. 20). Results of this uncertainty for precipitation change signal indicate that all changes except for wet season can be considered robust.

4. Discussion and conclusions

In this study, RegCM4.4 regional climate model's ability to reproduce the observed climatology over the Middle East – North Africa (MENA) CORDEX domain is investigated by forcing regional model with two different global datasets for four climatological seasons (DJF, MAM, JJA and SON). Performance of models in simulating present temperature and precipitation climatology of domain is evaluated by comparing the ERA-Interim reanalysis dataset for the period of 1980–2000 and the CRU observational dataset for the period of 1970–2000 with the output of global climate models of HadGEM2-ES and MPI-ESM-MR for the period of 1970–2000 as an input to the regional climate model. We run regional climate model RegCM with RCP4.5 and RCP8.5 emission scenario output of forcing data of HadGEM2-ES and MPI-ESM-MR for near future (2010–2040), mid-future (2040–2070) and far future (2070–2100) periods. Results show that the RegCM regional model sufficiently reproduced the observed temperature climatology of dry regions with an overall temperature bias of model between −3.0 and 3.0 °C. The similar spatial pattern of

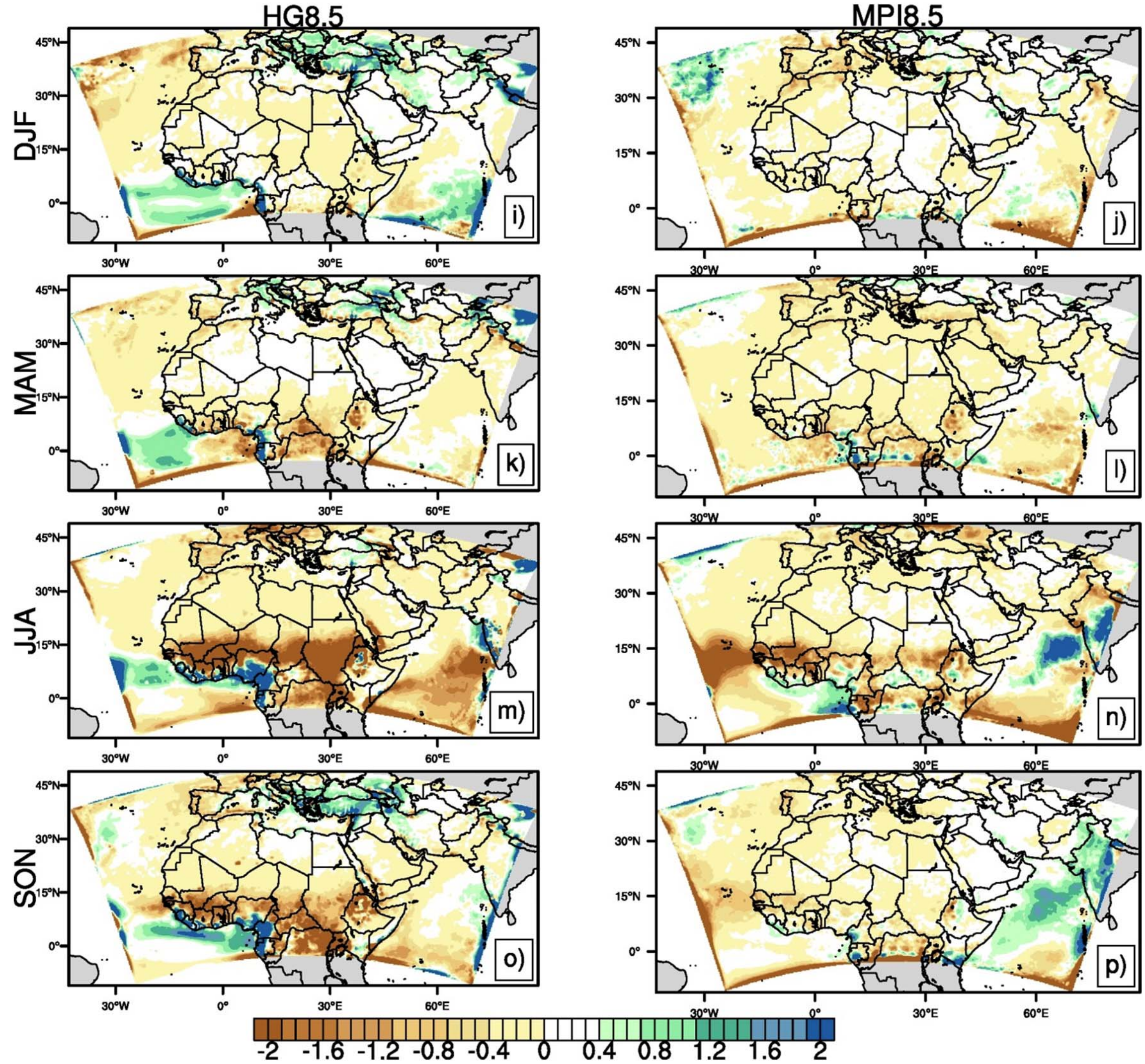

Fig. 17. Same as Fig. 15, but for the period of 2040–2070.

bias is also found by Almazroui et al. (2016). Precipitation amounts were overestimated by regional model in almost all parts of the domain for all seasons except the Sahara the Great Desert, the Western Sahara, and the Sahel regions, which are characterized by hyper-arid/arid and semiarid ecological and climatic conditions. However, the overestimation in precipitation compatibly support the recommendation that the pair of BATS land-use scheme and Grell scheme with the Fritsch-Chappell type closure is superior to the alternative land-surface scheme and convection parameterization pairs (Almazroui, 2016). In order to reduce the precipitation bias, the treatment of aerosols could be very beneficial considering the crucial role of direct and indirect impacts of dust transportation from the Sahel region and the Arabian Peninsula (Choobari et al., 2014), especially in summer (Konare et al., 2008; Nabat et al., 2012; Solmon et al., 2008). Moreover, the lack of the radiative effects of mineral aerosols can result in cold biases as well (Ji et al., 2015, 2016a, b; Zittis and Hadjinicolaou, 2017). Without the treatment of aerosols, the performance of the RegCM might be found insufficient in terms of improving the GCMs' performance. According to Panitz et al. (2014) and Dosio et al. (2015), the increase of the model resolution does not usually bring evident improvements to the results. The beginning of the rainy monsoon season over the West Africa is associated with the northward shift of the Inter Tropical Convergence Zone (ITCZ), which makes the West African climate humid rainy during the summer season. According to model results of future projections, there will be an increase in air temperatures and decrease in precipitation amounts over the parts of the domain climatically controlled by the West African monsoon system except Nigeria and Cameroon. Future increase in precipitation is observed only over the Atlantic Ocean instead of land surfaces. Projection results show that the southward shift of the ITCZ will likely occur in the future. Consequently, warmer and drier conditions are expected to occur over the West Africa. A decrease in future summer precipitation amounts is hazardous for many developing countries, such as Somalia, which is already vulnerable in terms of drought and lower gross domestic product (GDP), since summer precipitation is very crucial for African domain. Strong decrease in precipitation amounts will likely occur over the South-European countries for summer season, especially for those having a coast on the Mediterranean Sea except north-western part of Turkey and the Black Sea Basin (i.e. Figs. 18e,f and 19m,n). During winter, this decrease can be associated with increased and larger-area effect of the subtropical Azores high pressure system over region, less southward shifting of mid-latitude cyclones originating from the

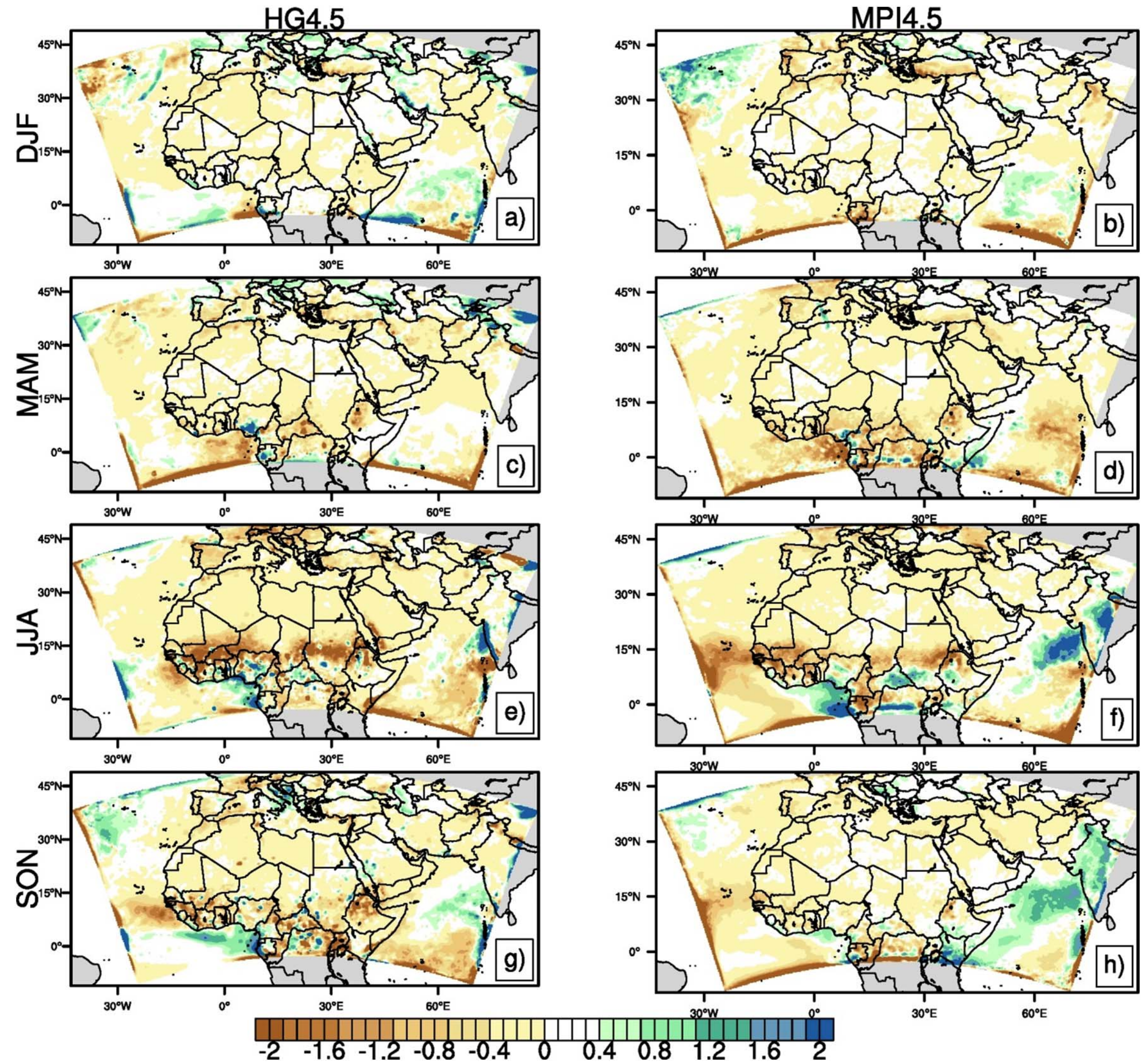

Fig. 18. Same as Fig. 16, but for the period of 2070–2100.

Northeast Atlantic and Iceland regions and decrease in frequency of Mediterranean originated cyclones. It may also be related to northward shift of the Iceland originated frontal cyclones and the Azores high pressure, and increase in frequency of positive phase of the North Atlantic Oscillation (NAO) variability over the Mediterranean Basin (Keuler et al., 2016; Mariotti et al., 2015; Trigo et al., 2006; Türkeş and Erlat, 2003, 2005; Zappa et al., 2015).

On the other hand, an increase in precipitation amounts during winter season is expected over the Black Sea Basin and the Caspian Sea probably because of an increased northerly circulation and mid-latitude cyclones over the Black Sea Basin and the Caspian Sea and being less stable with more moisture content. The humid/rainy and warmer than the long-term conditions generally occur in the Mediterranean Basin and surrounding regions due to increased frequency of mid-latitude and Mediterranean cyclones associated with increased west to south-westerly circulation types during the negative phase of NAO variability especially for winter season (Türkeş and Erlat, 2003, 2006, 2009; etc.). However, projection results show that the frequency of the negative phase of NAO will decrease (López-Moreno et al., 2011). This may affect hydrology and water resources systems of the Mediterranean Basin including increased frequency of water shortages and droughts. The projection results show that the increase in air temperatures over the domain will be from 3 °C up to 9 °C on average for the period of 2070–2100. This means that Evans' prediction of almost 4-degree warming in the Middle East at the end of this century (Evans, 2009) will double under the pessimistic RCP emission scenario. In addition, the projected increase in average temperatures supports the expectation of an increase of up to 7° in maximum temperatures (Lelieveld et al., 2016). Also, an increase in the number of strong heat extreme events will be observed as well (Lelieveld et al., 2016). According to output of regional model forced by scenario output of two global models, a strong decrease in the amounts of precipitation is also expected over most parts of the region in the future. These results are also in good agreement with the earlier studies, which expect an extremely hot and drier climate in the Middle East and North Africa (Evans, 2009, 2010; Lelieveld et al., 2016; Paeth et al., 2009; Radhouane, 2013). Therefore, the projected strong warming and drought (decrease in precipitation) conditions will very likely affect the CORDEX-MENA domain, which has already mostly hyper-arid, arid, semiarid and dry sub-humid climate and environment, and this makes the domain extremely vulnerable to climate change, particularly to increased droughts, bush and forest fires.

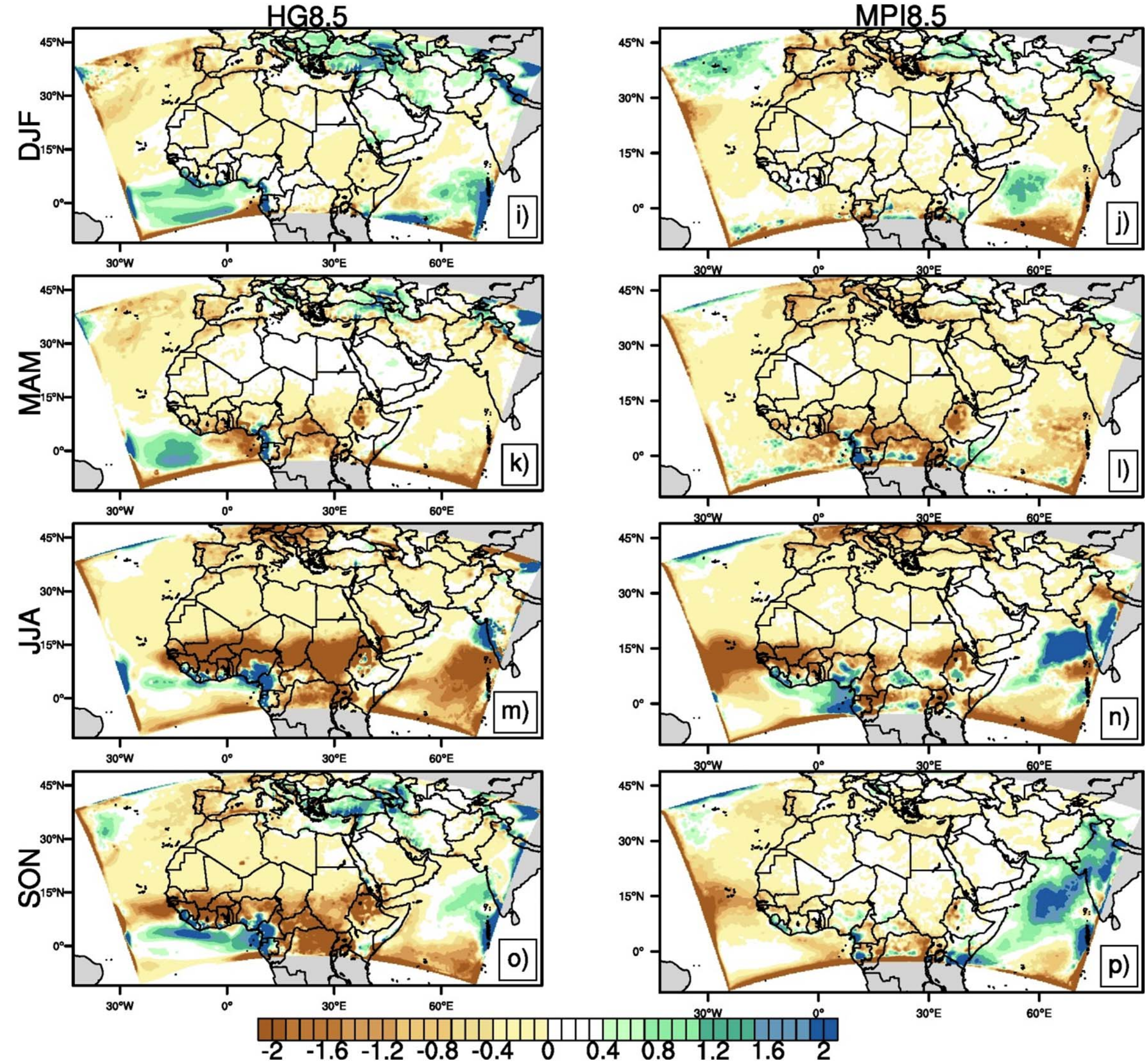

Fig. 19. Same as Fig. 17, but for the period of 2070–2100.

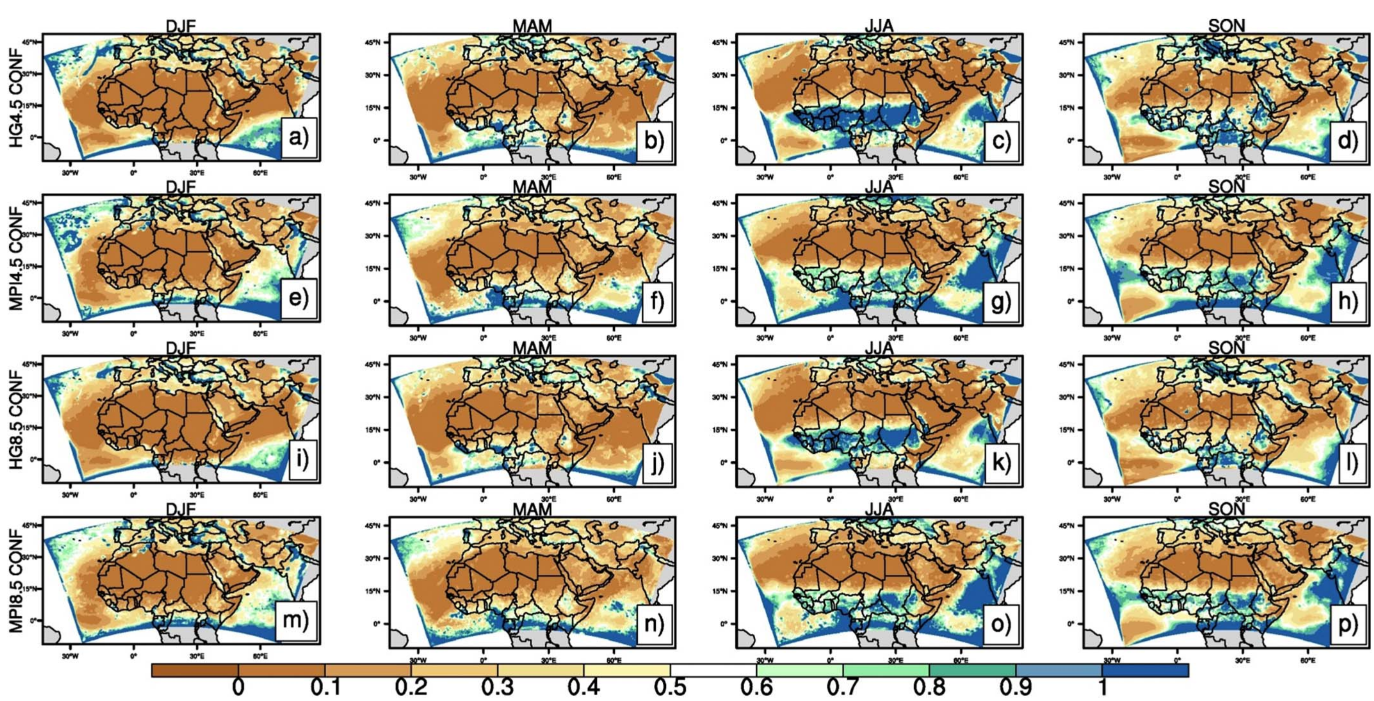

Fig. 20. The 95 percentile confidence range values for precipitation (mm/day) change obtained for RegCM4.4 simulations with (a–d) HadGEM2-ES (RCP4.5), (e–h) MPI-ESM-MR (RCP4.5), (i–l) HadGEM2-ES (RCP8.5), (m–p) MPI-ESM-MR (RCP8.5) for the period of 2070–2100 with respect to the period of 1970–2000.

Acknowledgements

We thank Abdullah Akbas of Ardahan University for his valuable comments. This work has been supported by Bogazici University BAP under Project Number 13561.

References

Adloff, F., Somot, S., Sevault, F., Jordà, G., Aznar, R., Déqué, M., Herrman, M., Marta, M., Dubois, C., Padorno, E., Alvarez-Fanjul, E., Gomis, D., 2015. Mediterranean Sea response to climate change in an ensemble of twenty first century scenarios. Clim. Dyn. 45, 2775–2802. http://dx.doi.org/10.1007/s00382-015-2507-3.

Almazroui, M., 2012. Dynamical downscaling of rainfall and temperature over the Arabian Peninsula using RegCM4. Clim. Res. 52, 49–62. http://dx.doi.org/10.3354/cr01073.

Almazroui, M., 2016. RegCM4 in climate simulation over CORDEX-MENA/Arab domain: selection of suitable domain, convection and land-surface schemes. Int. J. Climatol. 36, 236–251. http://dx.doi.org/10.1002/joc.4340.

Almazroui, M., Islam, M.N., Al-Khalaf, A.K., Saeed, F., 2015. Best convective parametrization scheme within RegCM4 to downscale CMIP5 multi-model data for the CORDEX-MENA/Arab domain. Theor. Appl. Climatol. 124, 807–823.

Almazroui, M., Islam, M.N., Alkhalaf, A.K., Saeed, F., Dambul, R., Rahman, M.A., 2016. Simulation of temperature and precipitation climatology for the CORDEX-MENA/Arab domain using RegCM4. Arab. J. Geosci. 9 (1), 1–13.

Almazroui, M., Islam, M.N., Balkhair, K.S., Şen, Z., Masood, A., 2017. Rainwater harvesting possibility under climate change: a basin-scale case study over western province of Saudi Arabia. Atmos. Res. 189, 11–23.

Alpert, P., Krichak, S.O., Shafir, H., Haim, D., Osetinsky, I., 2008. Climatic trends to extremes employing regional modeling and statistical interpretation over the E. Mediterranean. Glob. Planet. Chang. 63, 163–170.

Arnell, N.W., 2004. Climate change and global water resources: SRES emissions and socio-economic scenarios. Glob. Environ. Chang. 14 (1), 31–52.

Bucchignani, E., Cattaneo, L., Panitz, H.J., Mercogliano, P., 2016. Sensitivity analysis with the regional climate model COSMO-CLM over the CORDEX-MENA domain. Meteorog. Atmos. Phys. 128, 73–95.

Chen, M., Pollard, D., Barron, E.J., 2003. Comparison of future climate change over North America simulated by two regional models. J. Geophys. Res.-Atmos. 108 (D12), 4348. http://dx.doi.org/10.1029/2002JD002738.

Choobari, O.A., Zawar-Reza, P., Sturman, A., 2014. The global distribution of mineral dust and its impacts on the climate system: a review. Atmos. Res. 138, 152–165.

Conway, D., Hulme, M., 1996. The impacts of climate variability and future climate change in the Nile Basin on water resources in Egypt. Int. J. Water Resour. Dev. 12 (3), 277–296.

Coppola, E., Giorgi, F., Raffaele, F., Fuentes-Franco, R., Giuliani, G., Llopart-Pereira, M., Mamgain, A., Mariotti, L., Diro, G.T., Torma, C., 2014. Present and future climatologies in the phase I CREMA experiment. Clim. Chang. 125 (1), 23–38.

Dickinson, R.E., Kennedy, P.J., Henderson-Sellers, A., 1993. Biosphere-Atmosphere Transfer Scheme (BATS) Version 1e as Coupled to the NCAR Community Climate Model. National Center for Atmospheric Research, Climate and Global Dynamics Division.

Dosio, A., Panitz, H.J., Schubert-Frisius, M., Lüthi, D., 2015. Dynamical downscaling of CMIP5 global circulation models over CORDEX-Africa with COSMO-CLM: evaluation over the present climate and analysis of the added value. Clim. Dyn. 44 (9–10), 2637–2661.

Endris, H.S., Lennard, C., Hewitson, B., Dosio, A., Nikulin, G., Panitz, H.J., 2015. Teleconnection responses in multi-GCM driven CORDEX RCMs over Eastern Africa. Clim. Dyn. 46 (9–10), 2821–2846.

Erlat, E., Türkeş, M., 2013. Observed changes and trends in numbers of summer and tropical days, and the 2010 hot summer in Turkey. Int. J. Climatol. 33 (8), 1898–1908.

Erlat, E., Türkeş, M., 2017. Observed variations and trends in number of tropical nights in Turkey. Aegean Geogr. J. 26 (2), 95–106 (in Turkish with an English abstract, figure and table captions).

Evans, J.P., 2009. 21st century climate change in the Middle East. Clim. Chang. 92 (3–4), 417–432.

Evans, J.P., 2010. Global warming impact on the dominant precipitation processes in the Middle East. Theor. Appl. Climatol. 99 (3–4), 389–402.

Evans, J.P., 2011. CORDEX–An international climate downscaling initiative. In: Chan, F., Marinova, D., Anderssen, R.S. (Eds.), MODSIM2011, 19th International Congress on Modelling and Simulation. Modelling and Simulation Society of Australia and New Zealand, December 2011, pp. 2705–2711 (ISBN: 978-0-9872143-1-7).

Fritsch, J.M., Chappell, C.F., 1980. Numerical prediction of convectively driven mesoscale pressure systems. Part I: convective parameterization. J. Atmos. Sci. 37 (8), 1722–1733.

Gao, X., Giorgi, F., 2008. Increased aridity in the Mediterranean region under greenhouse gas forcing estimated from high resolution regional climate projections. Glob. Planet. Chang. 62, 195–209.

Gao, X., Zhao, Z., Giorgi, F., 2002. Changes of extreme events in regional climate simulations over East Asia. Adv. Atmos. Sci. 19 (5), 927–942.

Giorgi, F., 2006. Climate change hot-spots. Geophys. Res. Lett. 33, L08707. http://dx.doi.org/10.1029/2006GL025734.

Giorgi, F., 2014. Introduction to the special issue: the phase I CORDEX RegCM4 hypermatrix (CREMA) experiment. Clim. Chang. 125 (1), 1–5.

Giorgi, F., Lionello, P., 2008. Climate change projections for the Mediterranean region. Glob. Planet. Chang. 63 (2), 90–104.

Giorgi, F., Bi, X., Pal, J., 2004a. Mean interannual variability and trends in a regional climate change experiment over Europe. I. Present-day climate (1961–1990). Clim. Dyn. 22 (6–7), 733–756.

Giorgi, F., Bi, X., Pal, J., 2004b. Mean interannual variability and trends in a regional climate change experiment over Europe. II: climate change scenarios (2071–2100). Clim. Dyn. 23 (7–8), 839–858.

Giorgi, F., Jones, C., Asrar, G.R., 2009. Addressing climate information needs at the regional level: the CORDEX framework. In: World Meteorological Organization (WMO) Bulletin. 58(3). pp. 175.

Giorgi, F., Coppola, E., Solmon, F., Mariotti, L., Sylla, M.B., Bi, X., Elguindi, N., Diro, G.T., Nair, V., Giuliani, G., Turuncoglu, U.U., Cozzini, S., Güttler, I., O'Brien, T.A., Tawfik, A.B., Shalaby, A., Zakey, A.S., Steiner, A.L., Stordal, F., Sloan, L.C., Brankovic, C., 2012. RegCM4: model description and preliminary tests over multiple CORDEX domains. Clim. Res. 52, 7–29.

Giorgi, F., Coppola, E., Raffaele, F., Diro, G.T., Fuentes-Franco, R., Giuliani, G., Mamgain, A., Llopart, M.P., Mariotti, L., Torma, C., 2014. Changes in extremes and hydroclimatic regimes in the CREMA ensemble projections. Clim. Chang. 125 (1), 39–51.

Grell, G.A., 1993. Prognostic evaluation of assumptions used by cumulus parameterizations. Mon. Weather Rev. 121 (3), 764–787.

Gu, H., Wang, G., Yu, Z., Mei, R., 2012. Assessing future climate changes and extreme indicators in east and south Asia using the RegCM4 regional climate model. Clim. Chang. 114 (2), 301–317.

Hertig, E., Jacobeit, J., 2008. Downscaling future climate change: temperature scenarios for the Mediterranean area. Glob. Planet. Chang. 63 (2), 127–131.

Hulme, M., Doherty, R., Ngara, T., New, M., Lister, D., 2001. African climate change: 1900–2100. Clim. Res. 17 (2), 145–168.

IPCC, 2013a. In: Stocker, T.F., Qin, D., Plattner, G.-K., Tignor, M., Allen, S.K., Boschung, J., Nauels, A., Xia, Y., Bex, V., Midgley, P.M. (Eds.), Climate Change 2013: The Physical Science Basis. Contribution of Working Group I to the Fifth Assessment Report of the Intergovernmental Panel on Climate Change. Cambridge University Press, Cambridge (1535 pp).

IPCC, 2013b. Annex I: atlas of global and regional climate projections. In: van Oldenborgh, G.J., Collins, M., Arblaster, J., Christensen, J.H., Marotzke, J., Power, S.B., Rummukainen, M., Zhou, T. (Eds.), Climate Change 2013: The Physical Science Basis. Contribution of Working Group I to the Fifth Assessment Report of the Intergovernmental Panel on Climate Change. Cambridge University Press, Cambridge, United Kingdom and New York, NY, USA (Stocker TF, Qin D, Plattner G-K, Tignor M, Allen SK, Boschung J, Nauels A, Xia Y, Bex V, Midgley PM. (Eds.)).

Ji, Z., Kang, S., 2013. Double-nested dynamical downscaling experiments over the Tibetan plateau and their projection of climate change under two RCP scenarios. J. Atmos. Sci. 70 (4), 1278–1290.

Ji, Z., Wang, G., Yu, M., Pal, J.S., 2015. Potential climate effect of mineral aerosols over West Africa: part II—contribution of dust and land cover to future climate change. Clim. Dyn. 1–19. http://dx.doi.org/10.1007/s00382-015-2792-x.

Ji, Z., Kang, S., Zhang, Q., Cong, Z., Chen, P., Sillanpää, M., 2016a. Investigation of mineral aerosols radiative effects over High Mountain Asia in 1990–2009 using a regional climate model. Atmos. Res. 178, 484–496.

Ji, Z., Wang, G., Pal, J.S., Yu, M., 2016b. Potential climate effect of mineral aerosols over West Africa. Part I: model validation and contemporary climate evaluation. Clim. Dyn. 46 (3–4), 1223–1239.

Keuler, K., Radtke, K., Kotlarski, S., Lüthi, D., 2016. Regional climate change over Europe in COSMO-CLM: influence of emission scenario and driving global model. Meteorol. Z. 25, 121–136.

Konare, A., Zakey, A.S., Solmon, F., Giorgi, F., Rauscher, S., Ibrah, S., Bi, X., 2008. A regional climate modeling study of the effect of desert dust on the West African monsoon. J. Geophys. Res.-Atmos. 113, D12206. http://dx.doi.org/10.1029/2007JD009322.

Kuglitsch, F.G., Toreti, A., Xoplaki, E., Della-Marta, P.M., Zerefos, C.S., Türkeş, M., Luterbacher, J., 2010. Heat wave changes in the eastern Mediterranean since 1960. Geophys. Res. Lett. 37, L04802. http://dx.doi.org/10.1029/2009GL041841.

Kutiel, H., Türkeş, M., 2017. Spatial and temporal variability of dryness characteristics in Turkey. Int. J. Climatol. 37 (Suppl.1), 818–828. http://dx.doi.org/10.1002/joc.5040.

Laprise, R., Hernández-Díaz, L., Tete, K., Sushama, L., Šeparović, L., Martynov, A., Winger, K., Valin, M., 2013. Climate projections over CORDEX Africa domain using the fifth-generation Canadian Regional Climate Model (CRCM5). Clim. Dyn. 41 (11 − 12), 3219–3246.

Lelieveld, J., Hadjinicolaou, P., Kostopoulou, E., Chenoweth, J., Giannakopoulos, C., Hannides, C., Lange, M.A., El Maayar, M., Tanarthe, M., Tyrlis, E., Xoplaki, E., 2012. Climate change and impacts in the eastern Mediterranean and the Middle East. Clim. Chang. 114, 667–687.

Lelieveld, J., Hadjinicolaou, P., Kostopoulou, E., Giannakopoulos, C., Pozzer, A., Tanarhte, M., Tyrlis, E., 2014. Model projected heat extremes and air pollution in the eastern Mediterranean and Middle East in the twenty-first century. Reg. Environ. Chang. 14 (5), 1937–1949.

Lelieveld, J., Proestos, Y., Hadjinicolaou, P., Tanarhte, M., Tyrlis, E., Zittis, G., 2016. Strongly increasing heat extremes in the Middle East and North Africa (MENA) in the 21st century. Clim. Chang. 137 (1), 245–260.

López-Moreno, J.I., Vicente-Serrano, S.M., Morán-Tejeda, E., Lorenzo-Lacruz, J., Kenawy, A., Beniston, M., 2011. Effects of the North Atlantic Oscillation (NAO) on combined temperature and precipitation winter modes in the Mediterranean mountains: observed relationships and projections for the 21st century. Glob. Planet. Chang. 77 (1), 62–76.

Maity, S., Satyanarayana, A.N.V., Mandal, M., Nayak, S., 2017. Performance evaluation of land surface models and cumulus convection schemes in the simulation of Indian

summer monsoon using a regional climate model. Atmos. Res. 197, 21–41.
Mariotti, L., Diallo, I., Coppola, E., Giorgi, F., 2014. Seasonal and intraseasonal changes of African monsoon climates in 21st century CORDEX projections. Clim. Chang. 125 (1), 53–65.
Mariotti, A., Pan, Y., Zeng, N., Alessandri, A., 2015. Long-term climate change in the Mediterranean region in the midst of decadal variability. Clim. Dyn. 44 (5), 1437–1456. http://dx.doi.org/10.1007/s00382-015-2487-3.
Nabat, P., Solmon, F., Mallet, M., Kok, J.F., Somot, S., 2012. Dust emission size distribution impact on aerosol budget and radiative forcing over the Mediterranean region: a regional climate model approach. Atmos. Chem. Phys. Discuss. 12 (7), 17835–17886.
Nikulin, G., Jones, C., Giorgi, F., Asrar, G., Büchner, M., Cerezo-Mota, R., Christensen, O.B., Déqué, M., Fernandez, J., Hänsler, A., Van Meijgaard, E., Samuelsson, P., Sylla, M.S., Sushama, L., 2012. Precipitation climatology in an ensemble of CORDEX-Africa regional climate simulations. J. Clim. 25 (18), 6057–6078.
Ozturk, T., Türkeş, M., Kurnaz, M.L., 2011. Analysing projected changes in future air temperature and precipitation climatology of Turkey by using RegCM4.3.5 climate simulations. Aegean Geogr. J. 20 (1), 17–27 (in Turkish with an English abstract, figure and table captions).
Ozturk, T., Altınsoy, H., Türkeş, M., Kurnaz, M.L., 2012. Simulation of temperature and precipitation climatology for central Asia CORDEX domain by using RegCM 4.0. Clim. Res. 52, 63–76.
Ozturk, T., Ceber, Z.P., Türkeş, M., Kurnaz, M.L., 2015. Projections of climate change in the Mediterranean Basin by using downscaled global climate model outputs. Int. J. Climatol. 35, 4276–4292. http://dx.doi.org/10.1002/joc.4285.
Ozturk, T., Turp, M.T., Türkeş, M., Kurnaz, M.L., 2017. Projected changes in temperature and precipitation climatology of Central Asia CORDEX region 8 by using RegCM4.3.5. Atmos. Res. 183, 296–307. http://dx.doi.org/10.1016/j.atmosres.2016.09.008.
Paeth, H., Born, K., Girmes, R., Podzun, R., Jacob, D., 2009. Regional climate change in tropical and northern Africa due to greenhouse forcing and land use changes. J. Clim. 22 (1), 114–132.
Pal, J.S., Giorgi, F., Bi, X., Elguindi, N., Solmon, F., Rauscher, S.A., Gao, X., Francisco, R., Zakey, A., Winter, J., Ashfaq, M., Syed, F.S., Sloan, L.C., Bell, J.L., Diffenbaugh, N.S., Karmacharya, J., Konaré, A., Martinez, D., Da Rocha, R.P., Steiner, A.L., 2007. Regional climate modeling for the developing world: the ICTP RegCM3 and RegCNET. Bull. Am. Meteorol. Soc. 88 (9), 1395–1409.
Panitz, H.J., Dosio, A., Büchner, M., Lüthi, D., Keuler, K., 2014. COSMO-CLM (CCLM) climate simulations over CORDEX-Africa domain: analysis of the ERA-interim driven simulations at 0.44 and 0.22 resolution. Clim. Dyn. 42 (11–12), 3015–3038.
Peel, M.C., Finlayson, B.L., McMahon, T.A., 2007. Updated world map of the Köppen-Geiger climate classification. Hydrol. Earth Syst. Sci. 11 (5), 1633–1644.
Radhouane, L., 2013. Climate change impacts on north African countries and on some Tunisian economic sectors. J. Agric. Environ. Int. Dev. 107 (1), 101–113.
Salih, A.A.M., Elagib, N.A., Tjernström, M., Zhang, Q., 2018. Characterization of the Sahelian-Sudan rainfall based on observations and regional climate models. Atmos. Res. 202, 205–218.
Sánchez, E., Gallardo, C., Gaertner, M.A., Arribas, A., Castro, M., 2004. Future climate extreme events in the Mediterranean simulated by a regional climate model: a first approach. Glob. Planet. Chang. 44 (1), 163–180.
Solmon, F., Mallet, M., Elguindi, N., Giorgi, F., Zakey, A., Konaré, A., 2008. Dust aerosol impact on regional precipitation over western Africa, mechanisms and sensitivity to absorption properties. Geophys. Res. Lett. 35, L24705. http://dx.doi.org/10.1029/2008GL035900.
Somot, S., Sevault, F., Déqué, M., Crépon, M., 2008. 21st century climate change scenario for the Mediterranean using a coupled atmosphere–ocean regional climate model. Glob. Planet. Chang. 63 (2), 112–126.
Sowers, J., Vengosh, A., Weinthal, E., 2011. Climate change, water resources, and the politics of adaptation in the Middle East and North Africa. Clim. Chang. 104 (3–4), 599–627.
Sylla, M.B., Pal, J.S., Wang, G.L., Lawrence, P.J., 2016. Impact of land cover characterization on regional climate modeling over West Africa. Clim. Dyn. 46 (1–2), 637–650.
Tanarhte, M., Hadjinicolaou, P., Lelieveld, J., 2015. Heat wave characteristics in the Eastern Mediterranean and Middle East using extreme value theory. Clim. Res. 63 (2), 99–113.
Taylor, K.E., Stouffer, R.J., Meehl, G.A., 2012. An overview of CMIP5 and the experiment design. Bull. Am. Meteorol. Soc. 93 (4), 485–498.
Topcu, S., Sen, B., Türkeş, M., 2010. Observed and projected changes in drought conditions of Turkey. In: Options Méditerranéennes. Series A, Mediterranean Seminars 2010, Economies of Drought and Drought Preparedness in a Climate Change Contextpp. 123–127.
Tramblay, Y., Ruelland, D., Somot, S., Bouaicha, R., Servat, E., 2013. High-resolution Med-CORDEX regional climate model simulations for hydrological impact studies: a first evaluation of the ALADIN-climate model in Morocco. Hydrol. Earth Syst. Sci. 17, 3721–3739.
Trigo, R., Xoplaki, E., Zorita, E., Luterbacher, J., Krichak, S., Alpert, P., Jacobeit, J., Saenz, J., Fernandez, J., Gonzalez-Rouco, F., Garcia-Herrera, R., Rodo, X., Brunetti, M., Nanni, T., Maugeri, M., Türkeş, M., Gimeno, L., Ribera, P., Brunet, M., Trigo, I., Crepon, M., Mariotti, A., 2006. Relations between variability in the Mediterranean region and mid-latitude variability. In: Lionello, P., Malanotte-Rizzoli, P., Boscolo, R. (Eds.), Mediterranean Climate Variability. Elsevier Developments in Earth & Environmental Sciences 4, Amsterdam, pp. 179–226.
Türkeş, M., 2017. General climatology: fundamentals of atmosphere, weather and climate. Kriter Publisher Physical Geography Series No: 4 Kriter Publisher, İstanbul (Revised Second Edition, In Turkish, ISBN: 978-605-9336-28-4, xxiv + 520 pp).
Türkeş, M., Erlat, E., 2003. Precipitation changes and variability in Turkey linked to the North Atlantic Oscillation during the period 1930–2000. Int. J. Climatol. 23, 1771–1796.
Türkeş, M., Erlat, E., 2005. Climatological responses of winter precipitation in Turkey to variability of the North Atlantic Oscillation during the period 1930–2001. Theor. Appl. Climatol. 81, 45–69.
Türkeş, M., Erlat, E., 2006. Influences of the North Atlantic Oscillation on precipitation variability and changes in Turkey. In: Nuovo Cimento Della Societa Italiana Di Fisica C-Geophysics and Space Physics. 29. pp. 117–135.
Türkeş, M., Erlat, E., 2009. Winter mean temperature variability in Turkey associated with the North Atlantic Oscillation. Meteorog. Atmos. Phys. 105, 211–225. http://dx.doi.org/10.1007/s00703-009-0046-3.
Türkeş, M., Kurnaz, M.L., Ozturk, T., Altinsoy, H., 2011. Climate changes versus ‘security and peace’ in the Mediterranean macroclimate region: are they correlated. In: In Proceedings of International Human Security Conference on Human Security: New Challenges, New Perspectives, pp. 625–639.
Turp, M.T., Ozturk, T., Türkeş, M., Kurnaz, M.L., 2014. Investigation of projected changes for near future air temperature and precipitation climatology of Turkey and surrounding regions by using the regional climate model RegCM4.3.5. Aegean Geogr. J.l 23 (1), 1–24 (in Turkish with an English abstract, figure and table captions).
Turp, M.T., Ozturk, T., Türkeş, M., Kurnaz, M.L., 2015. Assessment of projected changes in air temperature and precipitation over the Mediterranean region via multi-model ensemble mean of CMIP5 models. Journal of the Black Sea/Mediterranean. Environment 21, 93–96.
Van Vuuren, D.P., Edmonds, J., Kainuma, M., Riahi, K., Thomson, A., Hibbard, K., Hurtt, G.C., Kram, T., Krey, V., Lamarque, J.F., Masui, T., Meinshausen, M., Nakicenovic, N., Smith, S.J., Rose, S.K., 2011. The representative concentration pathways: an overview. Clim. Chang. 109, 5–31.
Zappa, G., Hoskins, B.J., Shepherd, T.G., 2015. The dependence of wintertime Mediterranean precipitation on the atmospheric circulation response to climate change. Environ. Res. Lett. 10, 104012.
Zhang, X., Aguilar, E., Sensoy, S., Melkonyan, H., Tagiyeva, U., Ahmed, N., Kutaladze, N., Rahimzadeh, F., Taghipour, A., Hantosh, T.H., Albert, P., Semawi, M., Ali, M.K., Al-Shabibi, M.H.S., Al-Oulan, Z., Zatari, T., Al Dean Khelet, I., Hamoud, S., Sagir, R., Demircan, M., Eken, M., Adiguzel, M., Alexander, L., Peterson, T.C., Wallis, T., 2005. Trends in Middle East climate extreme indices from 1950 to 2003. J. Geophys. Res.-Atmos. 110, D22104. http://dx.doi.org/10.1029/2005JD006181.
Zittis, G., Hadjinicolaou, P., 2017. The effect of radiation parameterization schemes on surface temperature in regional climate simulations over the MENA-CORDEX domain. Int. J. Climatol. 37 (10), 3847–3862.
Zittis, G., Hadjinicolaou, P., Lelieveld, J., 2014. Comparison of WRF model physics parameterizations over the MENA-CORDEX domain. Am. J. Clim. Chang. 3, 490–511.